Stiction Prevention in MEMS Structures After Wet Treatment by Optimized Drying Techniques

Pooya Laamerad

A Thesis

In

The Department

of

Electrical and Computer Engineering

Presented in Partial Fulfillment of Requirements
For the Degree of Master of Applied Science
(Electrical & Computer Engineering) at

Concordia University
Montreal, Quebec, Canada

July 2016

CONCORDIA UNIVERSITY

School of Graduate Studies

This is to certify that the thesis prepared

By: Pooya Laamerad

Entitled: Stiction Prevention in MEMS Structures After Wet Treatment by Optimized Drying Techniques

and submitted in partial fulfillment of the requirements for the degree of

Master of Applied Science

Complies with the regulations of this University and meets the accepted standards with respect to originality and quality.

Signed by the final Examining Committee:

_____Chair

Dr. Rabin Raut

_____Examiner

Dr. Asim J. Al-Khalili

_____Examiner

Dr. Christian Moreau

_____Supervisors

Dr. Mojtaba Kahrizi and Dr. Irina Stateikina

Approved _____

Chair of Department of Graduate Program Director

_____2016 _____

ABSTRACT

Stiction Prevention in MEMS Structures After Wet Treatment by Optimized Drying Techniques

Pooya Laamerad

The demand driven by applications of MEMS (Micro-Electro-Mechanical Systems), calls for smaller devices, which are produced in various shapes and geometries. This imposes significant strain on the fabrication procedure, often resulting in elevated costs. As one of the main fabrication techniques, wet etching is an attractive alternative to dry etching because of its low cost. However, in this method, for etching and/or cleaning of wafers, we use liquid chemicals, which may result in stiction of suspended structures. Thus, the drying process is being an essential step in wet processing. If we do not have a proper technique to evaporate liquid inside structures, stiction would be unavoidable and may cause failure in fabricated devices. Low Consumption IPA (IsoPropyl Alcohol) dryer (LuCID) is an innovative and fully automated drying tool. LuCID is a Marangoni style dryer that uses IPA to vaporize water on wafer surface and in cavities of the fabricated microdevices, followed by drying with heated N_2. With the assistance of Centre de Collaboration MiQro Innovation (C2MI) and Teledyne DALSA partnership, a set of test structures was fabricated in view of optimization of the drying procedure. These test wafers include ribbons and cantilevers with different sizes to test stiction under various conditions. Both surface and bulk micromachining methods were tested with most common structural materials, such as Low Stress Nitride (LSN) and In-Situ Doped Polysilicon (ISDP) layer. With changing LuCID parameters controlling amount and type of IPA injections drying cycle was optimized and the results of this study will be presented in this work. The influence of the liquid and solid surface tension on stiction has been investigated in this study. Moreover, by using LuCID after wet etching, we show that by adjusting the concentration of IPA injected during the drying process, it is possible to reduce stiction.

Acknowledgements

I would like to express a tremendous amount of gratitude and respect to my supervisors Dr. Mojtaba Kahrizi and Dr. Irina Stateikina for their unwavering support and encouragement during my study. Without their guidance this work would not have been possible.

The internship opportunity I had with Centre de Collaboration MiQro Innovation (C2MI) and Teledyne DALSA was a big milestone in my career development. I am grateful for having a chance to meet so many wonderful people and professionals who helped me during this internship period.

I also want to thank all my examination committee members for their time and their wonderful comments on my work.

I would like to thank my family, most importantly my parents and my brother, for their patience and love during these years. Thanks to all my friends who have added so many colors and cheers into my life.

And finally, my joy knows no bounds in expressing my cordial gratitude to my wife, Golia, because she is simply amazing.

Contents

List of Figures

List of Tables

Abbreviations

BOE	***B**uffered **O**xide **E**tch*
CMOS	***C**omplementary **M**etal-**O**xide-**S**emiconductor*
DHF	***D**iluted **H**ydrogen **F**luoride*
***DI** Water*	***De**ionized Water*
HF	***H**ydrogen **F**luoride*
IPA	***I**so**p**ropyl **A**lcohol*
ISDP	***I**n-**S**itu **D**oped **P**olysilicon*
LSN	***L**ow-**S**tress **N**itride*
LuCID	***L**ow **C**onsumption **I**PA **D**ryer*
MEMS	***M**icro-**E**lectro-**M**echanical **S**ystems*
PVDF	***P**oly-**V**inylidene **Di**fluoride*
RCWA	***R**igorous **C**oupled **W**ave **A**nalysis*
SC1	***S**tandard **C**leaning **1***
***STG** Dryer*	***S**urface **T**ension **G**radient Dryer*
TEOS	***T**etra**e**athyl **O**rtho**si**licate*
TMAH	***T**etra-**M**ethyl **A**mmonium **H**ydroxide*
XPS	***X**-ray **P**hotoelectron **S**pectroscopy*

Chapter 1 – Introduction and Literature Review

1.1 – Introduction

Scientists and engineers realized that reducing the size of electronic devices is necessary to improve the performance, functionality, and reliability of electrical device. More recently, the size of electrical devices has been decreased to scale of micro/nanometers and billion of them are fabricated on a single microchip.

Moreover, by improvement the technologies in all areas, the demand to provide mechanical structures and devices in smaller scale has increased sharply. This improvement leads us to new major trends in technology, referred to as micro- and nano-technology. Micro-Mechanical and Micro-Electrical devices are the key components in wide range of products such as sensors, measurement devices, medical applications, etc.. In addition, micro- and nano-technology is leading to great innovation in information and computer technologies, medicine, health and environment, power and energy systems, and transportation [1].

Semiconductor materials, such as silicon, play important roles for fabricating and manufacturing micro and nanostructures. Efforts are made to improve the manufacturing processes and equipment to miniaturize the scale of components and products. Taking to consideration the sensitivity of micro and nanostructures to any type of disturbance, various types of machines, devices, and robots are used during manufacturing. Still new and innovative ideas, devices and research are needed in micro and nanotechnology to reduce the cost of fabrication, improve functionality and increase performance and reliability. One of the challenges in fabrication of microelectromechanical systems (MEMS) is achieving successful release of micro-mechanical suspended structures by using wet chemical etching. To avoid stiction of released structures, design and optimization of drying tools is necessary after wet etching. One of the innovative tools used for drying micro devices is Low Consumption IPA Dryer (LuCID). In this work we have concentrated to investigate the benefits of LuCID

compared to other drying techniques. The aim of this study is to enhance the performance of this technique and its application in MEMS fabrication technology.

1.2 – MEMS (Micro-Electro-Mechanical Systems)

Micro-Electro-Mechanical System (MEMS) fabrication technology is technology of making small devices or systems in micrometers scale. It is the integration of elements of mechanical and electrical structures (e.g. sensors, actuators, and electronic circuits) on a substrate using microfabrication and micromachining processes technology. The microfabrication technology provides tools for batch processing of MEMS eliminating the need for discrete component assembly. Due to the multidisciplinary technology of MEMS, it has applications in many fields, including defence, aerospace, automotive, biomedical, and communication industries.

MEMS are widely used in many branches of electrical engineering. The progress of MEMS technology is very dependent on the development of mechanical actuating elements that are compatible with materials as well as processing technology. There are mainly two techniques used in industries to fabricate MEMS called bulk micromachining and surface micromachining.

Bulk micromachining is a popular silicon micromachining technology that is used to fabricate majority of commercial devices such as pressure sensors, micro valves, and accelerometers. The key factors in this technology are etching of a substrate using suitable etchants with specific selectivity properties. The etching could be done by bombarding the substrate with accelerated particles, it is called dry etching, or by dissolving the substrate in appropriate chemicals, it is called wet etching.

Surface micromachining is done by depositing structural thin films on top of sacrificial layers on the substrate (this could be done using standard CMOS technology) and then releasing the mechanical systems by etching said sacrificial layers. Usually, this is done using the wet etching. Wet etching is more popular due to its low cost and variety of chemical etchants. In many applications, various types of elements, e.g. cantilevers beams, membranes, used in MEMS, could be produced using either bulk or surface micromachining [2].

One of the steps in post processing in any MEMS technology, particularly after etching, is cleaning of the substrates with these structures. The cleaning step is designed to clean the surface of the structures and remove any contaminants from the surface and the spaces between suspended elements and the substrate, e.g. space between cantilevers and the substrate. Chemical clean is always followed by the rinse using DI water. Drying the devices, and removing water trapped between various layers of the structure is problematic due to the stiction or static frictions between the moving elements and substrate. It is essential to optimize the techniques to remove the water without damage to suspended structures. In order to understand the effect of stiction on MEMS processes, we first introduce the types and the reasons of stiction.

1.3 – Stiction

Failure of MEMS structures due to adhesion of contacting surfaces is a well-known issue. After etching and cleaning by means of wet etching, water droplets between two solid plates cause stiction [3]. In this section, we discuss the most important adhesive forces that operate between the surfaces. When the two surfaces are in vacuum or in air, the main interaction between them is the attractive van der Waals force [4]. However, when the surfaces, are entirely in liquid, the force between the surfaces is much more complex from that in vacuum or air. The van der Waals attraction is reduced, overshadowed by the other forces [4]. When water fills the area between the two surfaces, four interaction forces are present and could be described as follows:

1. **Capillary Force:** The main force that is responsible for adhesion between layers is. Capillary force is caused by the difference between the outside and the inside pressure of a water droplet. When a droplet is between two layers, the inside pressure of water droplet is lower than the outside pressure. This difference in pressures produces an attraction force between the surfaces, and as a result, stiction occurs between the layers [3]. The difference of pressure depends on the surface area of the wetted surface and the surface tension of the liquid-air interface. Therefore, the capillary force is related to the surface tension of liquid-air interface [4]:

$$F = \frac{2A\gamma_{la}\cos\theta_c}{D} \qquad (1)$$

Where A is the area of wetted surface, γ_{la} is the surface tension of the liquid-air interface, θ_c is the contact angle between liquid and solid, and D is the gap between two surfaces as is shown in Figure 1.1.

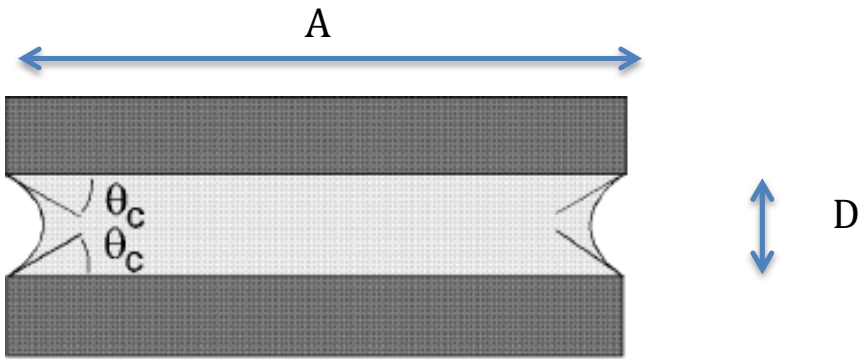

Figure 1. 1 A thin layer of liquid between two plates. $\boldsymbol{\theta_c}$ is the contact angle between liquid and solid in air. A is the wetted surface area and D is the gap between the layers [3].

The value of the contact angle is very important for capillary force. The contact angle depends on the surface tension of the solid-air (γ_{sa}), the surface tension of the solid-liquid (γ_{sl}) and the surface tension of the liquid-air (γ_{la}). The following equation shows the relation of contact angle and surface tension [5]:

$$\gamma_{sa} = \gamma_{sl} + \gamma_{la}\cos\theta_c \qquad 0 < \theta_c < \pi \qquad (2)$$

If the surface tension between substrate and air is smaller than the total surface tension of liquid-air and substrate-liquid, then the contact angle is larger than 0°[3]. In this situation the liquid droplet does not spread and remains between the surfaces as shown in Figure 1.2.

Figure 1. 2 When the contact angle is not zero ($0<\theta_c<90$), liquid makes a bridge between two solids, but it does not spread [3].

However, if the surface tension between substrate and air is bigger than the total surface tension of water-air and substrate-liquid, the contact angle becomes 0° and liquid spreads between layers and forms a thin water film at the surface of each substrate [3]. Figure 1.3 illustrates this situation.

Figure 1. 3 When the contact angle is zero ($\theta_c = 0$), Liquid makes a bridge between two solids, and spreads between layer [3].

The adhesion force when water spreads and covers the entire layer between two solids is higher than the adhesion when water does not spread [4]. In hydrophilic layers water spreads between layers and make a bridge across the layers. But even when the layers are hydrophobic, because the molecules of water are highly polar, the molecules of water at the meniscus turn over on the layers and spread along the layer [4].

2. **Electrostatic Force:** Water is highly polar liquid and when water is in contact with any surface, it creates the surface charge by detachment of ions from the surface [4]. This surface charge makes an adhesion force between layers, which is called electrostatic force.
3. In hydrophilic silicon surfaces, the hydrogen atoms of water trapped between silicon layers develop bonds between water's molecules. The silicon surfaces get hydrated and stick to each other [5]. This causes a small adhesion force in very thin structures [3], [5].
4. The other type of stiction occurs when water moves between layers. For example, when a wafer is submerged in water, water moves into the structures. Electron from water's

surface is transferred to the surface of silicon and causes electrical double layer at the surface of silicon [3]. The electrical layer that is produced between layers as a result of rubbing them on each other is a simpler and more familiar example for this situation. However, this electrical force is not able to make a permanent stiction, since the non-equilibrium charging will vanish after a while [3].

On the other hand, when the surfaces are dry, there are no ions or dipoles on the surfaces. The only attraction is just an interaction between atoms or molecules of each surface [4]. Therefore, instead of electrostatic force, van der Waals force is dominant.

The equation for the van der Waals force for two dry surfaces comes from the Lifshitz theory [4]. The equation is:

$$van\ der\ Waals\ interaction = \frac{-A_H}{6\pi D^3} \qquad (3)$$

A_H is Hamaker constant and depends on chemical structure of a surface [5]. D is the distance between two surfaces.

All these adhesion forces cause stiction. Various methods are used to reduce the stiction between layers. Injecting, dissolving, or spraying another liquid in water to reduce the surface tension of water is one of the methods to avoid stiction in wet situation. In this method, normally, IPA (Isopropyl Alcohol) is used to reduce the surface tension of water. In the following section the advantage of IPA will be discussed.

1.4 – IPA

Isopropyl Alcohol (IPA) with the chemical formula of C_3H_8O is a colorless flammable compound. To avoid stiction, drying wafer is essential after wet etching and wet cleaning. There are several techniques for drying wafers, and using IPA is very common in most of these techniques. There are various reasons for the usage of IPA in MEMS.

The first advantage of using IPA is to reduce the surface tension of water. So it is necessary to find the relationship between the concentration of IPA and the surface tension of water.

According to the research that has been done by Jin-Goo Park et al., as shown in Figure 1.4, the surface tension of water declines sharply by increasing the concentration of IPA [6].

Figure 1. 4 Relation between surface tension of water and IPA concentration. By increasing the concentration of IPA in water, the surface tension decreases [6].

Also IPA is very soluble in water. On the other hand, dissolving IPA in water increases adhesion force between particles and a silicon wafer. In the research of Jin-Goo Park et al., pure IPA is mixed with DI water in order to examine the adhesion force between silica particles and the silicon (Si) surface. Figure 1.5 shows their result. In this graph we may observe that by increasing the concentration of IPA in DI water, the adhesion force between silica particles and the silicon surface also increases.

Figure 1. 5 The adhesion force of silica particles and Si wafer with respect to the concentration of IPA. By increasing the concentration of IPA in DI water, the adhesion force between silica particles and the silicon surface also increases [6].

The above studies show that having IPA with higher concentration could reduce the surface tension of water. However, we should use IPA with lower concentration to avoid adhesion and reduce the electro-static interaction between particles and silicon wafer in a water-IPA solution. It means that it is necessary to find the specific value of IPA concentration to reduce the surface tension of water as well as to avoid any type of adhesion.
In addition, using IPA has another advantage. Introduction of IPA to DI wafer creates Marangoni effect, which will be described in the next section.

1.5 - The Marangoni Effect:

Marangoni effect happens when the surface tension of two phases (liquid-liquid) is different. There are two ways to change the surface tension of water. The first one is dissolving another liquid at the surface of water and the second one is changing the temperature of water at its interface with air [7]. When the Marangoni effect is only caused by the difference in surface tension, it is referred to as solute capillary effect, and when it is caused by difference in the

temperature, it is called thermo-capillary effect [8]. In this thesis, we focus on the Marangoni effect caused by the surface tension gradient. To obtain the surface tension gradient dissolving or spraying a liquid with lower surface tension such as IPA at the surface of water is a well-known method [7].

To understand Marangoni effect, first we need to define the capillary length. As mentioned earlier, capillary force makes the water droplet stick to the surface of wafer. When there is a water droplet on the surface of a wafer, the capillary force is dominant as long as the weight of water droplet is very small (the gravity force is very small). In other words, if the diameter of water droplet is smaller than the so-called Capillary Length (L_c), the capillary force will remain the dominant force and the droplet will stick to the surface. However, if the diameter of water droplet is larger than L_c, the gravity force will be stronger than the capillary force. In this case, the gravity will force the droplet to fall down [9]. L_c or the capillary length is given by the following equation:

$$L_c = \sqrt{\sigma/(\rho g)} \qquad (4)$$

where σ is the surface tension in N/m, ρ is the density of the fluid, and g is the acceleration of gravity. L_c for water is around 2.5 mm [10].

As an example, consider the case when after wet etching and cleaning, wafer is vertically submerged in the water tank and IPA from top of the water is vaporized at the surface of water. So at the surface of water there is a thin layer of IPA that spreads evenly. After that, the water is slowly drained out of the tank. This process creates a meniscus on the surface of wafer; see illustration in figure 1.6. IPA evaporates faster than water. When the IPA evaporates from the surface of water, the replacement is less probable at the meniscus in comparison with the area away from the wafer surface and meniscus identified in the Fig. 1.6(2) as area with the lower surface tension. Therefore, the concentration of IPA at the middle of the tank (the surface identified as lower surface tension area) is higher than the concentration of IPA at the meniscus; see illustration in figure 1.6(2), in the middle the surface tension is higher than the meniscus. A gradient of surface tension is produced as a result of the IPA evaporation and replacement rate. Because of this gradient, the surface tension at the meniscus would be higher than the surface tension at the middle of the tank. Since liquid prefers to flow from a surface with lower surface

tension to the one with higher surface tension, a flow of liquid occurs. This flow is called the Marangoni Flow and the whole process is called Marangoni effect. Figure 1.6 shows the process of Marangoni flow.

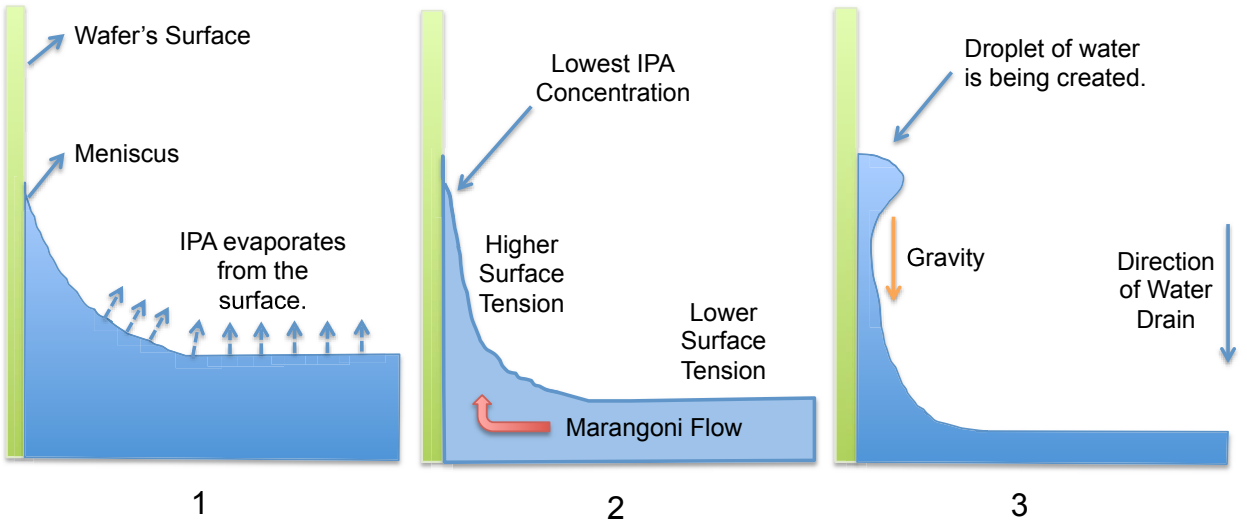

Figure 1. 6 The process of Marangoni flow. 1) A thin layer of IPA exists at the surface of water. The surface tension of water is decreased when an alcohol, such as IPA, is solved in or sprayed on the surface of the water. When water is rinsed down inside the tank, it makes a meniscus with the surface of the wafer. 2) When the IPA evaporates from the surface of the water, the rate of the replacement of IPA molecules at the meniscus is less than the one at the middle of the tank (lower surface tension area). Therefore, liquid moves from the surface with higher concentration of alcohol (lower surface tension area) to the surface with lower concentration of alcohol (higher surface tension area), shown as Marangoni flow. 3) Molecules of water tend to move to the top of the meniscus. As a result, a droplet of water is created. The droplet of water becomes larger until the gravity dominates and forces the droplet to fall down.

Because of Marangoni flow, water at top of the meniscus (higher surface tension) absorbs more water than the surface with lower surface tension and produces a droplet of water. The droplet of water becomes larger until gravity dominates and forces the droplet to fall down. This is the advantage of Marangoni effect. By gradient of surface tension, droplet of water absorbs surrounding water and eliminates watermarks on the substrate surface (removing watermarks from the surface of wafer is necessary to avoid any further failures).

As a conclusion, IPA is solvable in water, reduces the surface tension of water, and by creating Marangoni effect removes the water droplets on the surface of wafer after rinsing. Because of these properties, IPA is very popular for drying technique. There are various types of drying techniques and equipments exist to remove water from the surface of a wafer, and in most of them IPA is used. In the next section, three main drying techniques are described.

1.6 - Drying Techniques

Drying is essential in wet etching and cleaning processes. In wet etching and cleaning, chemical substances are used widely. Therefore, it is necessary to submerge and rinse a wafer in Deionized Water (DI water) after each chemical treatment.

However, after a wafer is taken out of the rinse tank, water remains in cavities or between the thin layers and membranes. This is one of the main reasons of stiction and failure in MEMS structures. Thus, drying is essential to reduce failures in MEMS. In this section three types of drying techniques will be introduced.

1.6.1 – Spin Dryer

One of the drying techniques used in microfabrication after wet etching is spin-drying. The wafer is placed on a plate inside a chamber. Normally, there is one or more holders to secure a plate, which keeps a sample wafer and these holders are connected to a rotor [11]. The rotor spins the secured wafer and the water droplets, present on the surface of wafer, are removed by centrifugal forces [11].

One of the main issues of this type of drying is a watermark. Usually, after drying wafers with this technique, a lot of watermarks remain on the surface of wafer [12]. The watermarks remaining after the drying by spin dryer are very critical for fabrication [13].

Furthermore, because of high speed of spin dryer there is a high chance of mechanical structures damage. With the current trends in the industry, the dimensions of structures are decreased to micro and nano sizes. So, the spinning during the drying process increases the probability of failure [13].

The main advantage of this technique is its low capital cost; however, as it was mentioned above, remaining watermarks are the main problem of this technique [13]. Besides, its mechanical handling is increasing the chance of damage to the devices on the wafer [13]. In general, this dryer is suitable only for low-tech MEMS structures.

1.6.2 – IPA Dryer

The other technique for drying is the Isopropyl Alcohol (IPA) Vapor Dryer technique. After wet etching or wet cleaning, the wetted wafer is placed in isopropyl alcohol zone (the red zone in Figure 1.7) [14] [15]. To make a sufficient amount of IPA's vapor, IPA liquid is heated at the bottom of the dryer's tank, and to maintain the amount of IPA as a vapor, electric heating panels are placed around the tank [15]. Normally, to prevent any contingence between heating facilities and IPA liquid, water-glycol is used to reduce the risk of fire [16].

At the bottom of the tank, IPA covers the wetted surface. Then, the wafers are moved to a cooler place which is normally located at the upper side of the inner tank to dry the whole substrate's surface [15]. In the topside of the tank (cooler side), liquid IPA is evaporated from the surface of wafer and it cleans the wafer as a result. IPA vapor dryer can be used as a stand-alone or in a row of tanks in any wet benches. Figure 1.7 shows the inner structure of IPA vapor dryer.

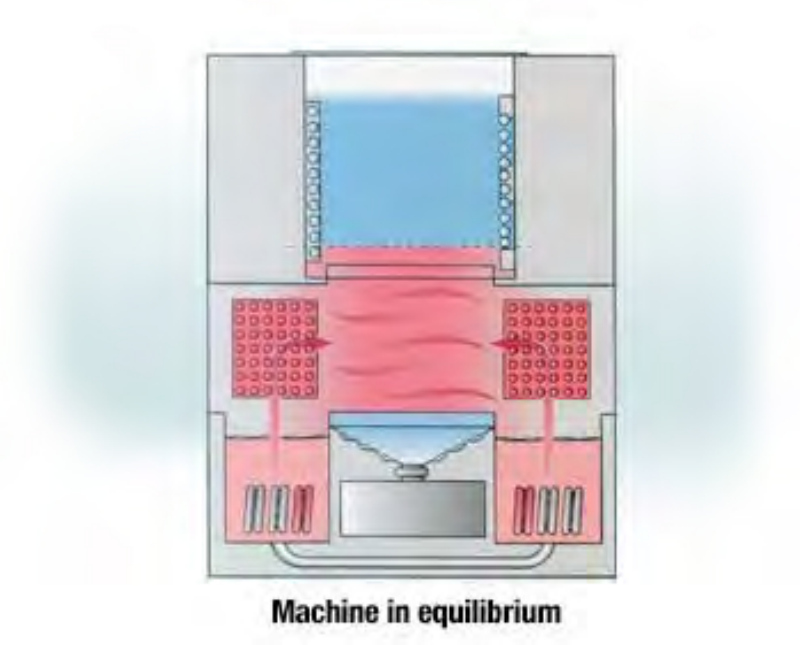

Figure 1.7 The IPA Vapor Dryer. At the bottom of the tank (red part), IPA is vaporized by heating facilities, and covers the wafer. Then, the wafer is covered with IPA and then is moved to the top of the tank (blue part). The blue part is a cooler part, and vapor IPA is changed to liquid IPA. The liquid IPA washes the surface and eliminates the remaining water [16].

The most important part in this device is the inner tank. The inner tank has to be designed for both hot and cold locations. Furthermore, this tank has to be made of stainless steel to reduce the

amount of contaminants that could be transferred from the inner tank to the surface of wafer especially at the hot part of the tank [15]. Finally, keeping the vapor concentration constant is very important in IPA vapor dryer. Besides, cooling system has to react quickly to dry the surface [15].

The first advantage of IPA dryer is its gentle wafer handling. The fact that it is also adoptable with all types of wet benches makes the IPA dryer a very promising technique. The results of drying with IPA dryer is much better than the ones with spin dryer [13]. However, the IPA dryer also has some disadvantages. One disadvantage is that the IPA dryer is significantly more expensive than the spin dryer. In addition, the IPA dryer increases the cost of manufacturing by consuming a large volume of IPA, as well as the drying process takes very long time [13]. In addition, the fire hazard and necessary safety procedures are considered as other disadvantages of IPA dryer.

1.6.3 – Marangoni Style Dryer

All Marangoni style dryers rely on mass transfer when the surface tension is different between two liquids [17]. Normally, IPA is used to make a gradient surface tension at the surface of water. Marangoni style dryer consists of an inner tank, containing the water and the outer tank with the lid. At first, wafer is submerged vertically in the inner tank, filled with DI water. The lid, containing nozzles for IPA injection on the surface of water, is closed. Holes at the bottom of the inner tank are designed to let the water flow out of the tank while the IPA is injected. IPA injections keep a sufficient layer of IPA at the top of water's surface during the time that water drains. When IPA is sprayed on top of the water surface, two fluids with different surface tensions are created at their interface (water and IPA). IPA can reduce the surface tension of water and make a surface tension gradient. As a result, Marangoni effect occurs since IPA evaporates faster than water. The process of drying a wafer was already described in the Marangoni Effect section.

This type of dryer has various names, such as Marangoni Dryer, Surface Tension Gradient Dryer (STG Dryer), Gradient Tension Dryer, and Low Consumption IPA Dryer (LuCID Dryer). In this study, LuCID Dryer, shown in Figure 1.8, is used as a type of Marangoni Style Dryer. In

the next section, the LuCID Dryer will be described and its advantages over other types of dryers are introduced.

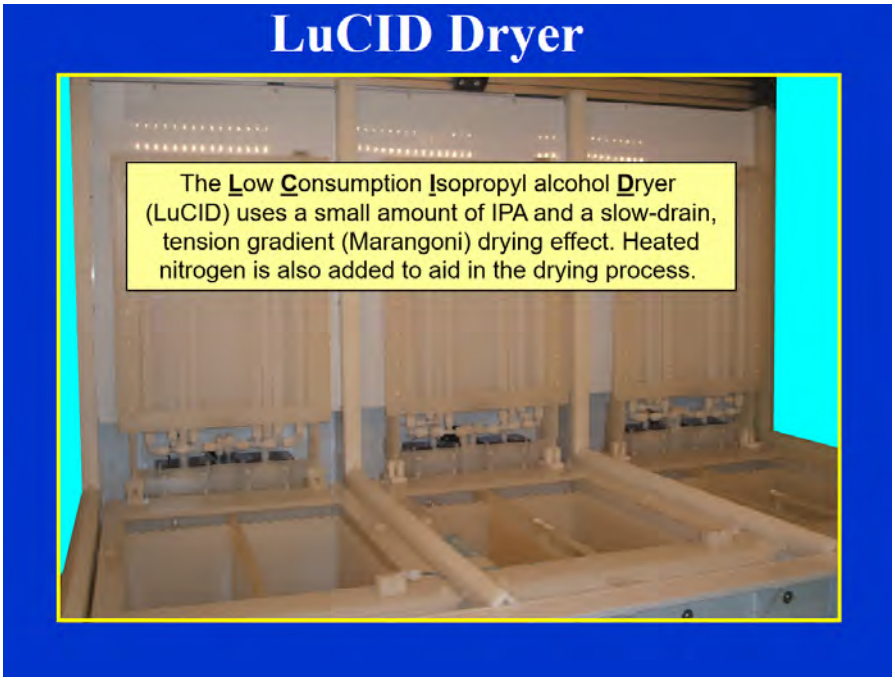

Figure 1. 8 Low Consumption Isopropyl alcohol Dryer (LuCID)

1.7 – Features and Benefits of LuCID Dryer

Low Consumption IPA Dryer (LuCID) is an innovative device for drying after wet etching and wet cleaning in MEMS manufacturing. As described earlier, this device uses Marangoni style drying to dry wafers. Before the drying sequence starts, an etched wafer is placed inside the rinse tank and after rinse cycle is complete, it is transferred into the LuCID Dryer.

LuCID consists of an inner tank, which is filled with DI water. Each time, before using LuCID the inner tank is filled with fresh DI water. At the bottom of LuCID Dryer, there are slow drain valves that are responsible for extracting water from the tank.

After wafer is submerged in the inner tank, the tank's lid is closed and the injection of IPA begins. The IPA injection nozzles are located on this lid. Water slowly drains inside the tank while the IPA is sprayed on the surface of water. Figure 1.9 illustrates all these sequences together.

Once, tank is completely drained, the IPA injection is stopped. In the final step, hot nitrogen is blown from the separate set of nozzles on the lid down to the wafer to complete the drying sequence and to evaporate any remaining liquid.

LuCID Dryer introduces a new way of using IPA for drying wafers and to remove the watermarks with Marangoni effect. This device is more effective than all other devices to remove watermarks. The results of spin drying show that the size of watermarks on wafers is around ten micron, however, the size of the remaining watermarks decrease to less than 1 micron when Marangoni style dryer is used [14]. In addition, in this technique, the risk of damage on the surface of wafer decreases since there is no movement during drying process. The other advantage of this drying method is that there is no mechanical stress on the substrate [14].

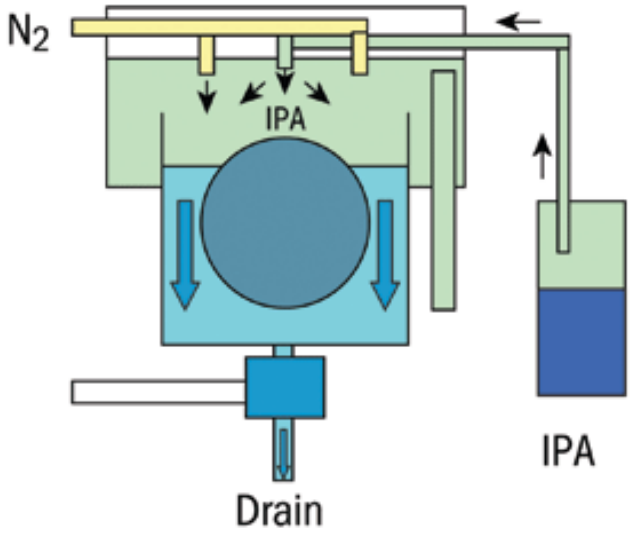

Figure 1. 9 The figure shows the schematic of LuCID. Wafer is submerged in the water. Then water rinses down from the drain valve at the bottom of the tank. During the rinse time, IPA is injected from the tank lid. After all IPA injections finish and all water extract from the tank, hot nitrogen flows to dry a wafer completely [18].

All Marangoni style dryers, such as LuCID Dryer, use IPA as the solvent in their devices. The complete miscibility of water with IPA makes perfect solution of water and IPA at the surface to have Marangoni effect [14]. However, the miscibility depends on the concentration of IPA. To have a better Marangoni effect at the surface, we need a uniformly mixture of IPA and water at

the surface of water. J.G. Park et al. have done a study on the surface excess of IPA at the air-water interface [6]. They define the surface excess as the difference between the amount of a component actually present in the system and that, which would be present in a reference system [19]. As an example, after IPA is vaporized on the surface of water, in the idealized situation, there would be one layer of uniformly mixed IPA and water mixture at the water/air interface. Therefore, there would be no surface excess [20]. In reality, there would be a non-uniformly spread layer of IPA/water mixture at the wafer/air interface [20]. Therefore, we have surface excess.

In drying process, it is desirable to have a lower value of surface excess to be able to have an equal amount of IPA and water molecules at the interface of these liquids. Figure 1.10 shows the change of surface excess at the interface of IPA and water with respect to the concentration of IPA [6].

Figure 1. 10 Surface excess as a function of IPA's concentration. The lowest amount of surface excess occurs when the concentration of IPA is lower than ~ 5 percent [6].

As illustrated in Figure 1.10, the highest surface excess occurs when the concentration of IPA is around 20 percent. By decreasing the concentration, the value of surface excess declines as well. The lowest amount of surface excess occurs when the concentration of IPA is lower than ~5 percent [6]. This is another reason to show that using a low concentration of IPA during the

drying process will provide complete mixture of IPA and water at the surface with low surface excess.

The concentration of IPA has direct effect on the absorption of contaminants. Figure 1.11 shows the magnitude of silica contaminants with respect to the concentration of IPA.

Figure 1. 11 Number of absorbed contaminants in respect to the concentration of IPA. The lowest number of absorbed contaminants occurs when the concentration of IPA is between 5 and 10 percent [6].

When the concentration of IPA is between 5 and 10 percent (also the surface excess is at the lowest range according to Figure 1.10) the number of absorbed contaminants is the lowest as well [6]. Figure 1.12 compares the concentration of metal contaminants at the surface of a wafer before and after of using Marangoni style dryer.

Table 1. 1 Comparison of surface contaminants before and after drying with Marangoni style dryer [17]. The figure shows the various types of metals. The number of atoms at the surface of wafer was measured before using Marangoni style dryer. Then the figure compares the number of atoms after cleaning and drying wafer with Marangoni style dryer.

Element	Spec Limit	Dryer Results
Al	50	6.3
Mg	5	2.9
Ca	40	18.7
K	5	0.1
Na	20	14.9
Cu	2	1.7
Fe	5	1.4
Ni	3	0.6
Zn	3	0.7
Cr	2	0.05

Selected Metal Contamination
VPD-ICP-MS Analysis
1 × E9 atoms/cm^2

In Table 1.1 the left column of the table illustrates the type of contaminants, the middle column shows the number of contaminants' particles per square centimeter on the surface before drying, and the right column contains the number of contaminants' particles per square centimetre on the surface after drying with IPA. Table 1.1 shows that IPA dryer can assist in removing contaminants from the surface of wafer after dying and reduce the amount of contaminants [17].

In summary, these works suggest that IPA with lower concentration is required to get better drying result when IPA is used for drying. This is the main reason that low consumption of IPA dryer was designed.

1.8 - Experimental work on Stiction

In the work that was done by C. H. Mastrangelo and C. H. Hsu, they calculated the final free and pinned state of cantilevers after wet etching. They divided the stiction process into two stages. The first stage happens by the capillary force, which is caused by a liquid, trapped between the surface of substrate and the released layer. This type of deflection is developed during the rinse-dry circle and is called collapse [21]. The magnitude of these forces is in some cases (depends on the physical properties of released structures) sufficient to deform and pin the released structures to the substrate. Collapse depends on liquid surface tension and the contact angle ($\gamma_l \cos\theta$). The second stage is the intersolid adhesion of the layer and the substrate [21]. If this intersolid adhesion is smaller than the deflection force of the cantilever, the cantilever will return, peel back, to its original suspended state [6]. Therefore, this stage is dependant on the solid surface tension (γ_s). Hence, stiction can be defined with two phenomena: the collapse and the intersolid adhesion [21] [22].

C. H. Mastrangelo and C. H. Hsu have found the theoretical equation for both mechanisms for cantilevers. To separate the suspended structures pinned to the substrate and peeled back states, they have defined two quantities for both types of adhesions. N_{EC} (elastocapillary number) is a criterion for the collapse type of adhesion. N_{EC} determines the boundary if the capillary pull is sufficient to reach contact with the substrate. N_p (peel number) is a criterion for the intersolid adhesion [21][23]. N_P determines the boundary if the intersolid adhesion can pin the cantilevers to the substrate. If N_{EC} and $N_p > 1$ the cantilever peels completely. In addition, when N_{EC} and $N_p < 1$ the cantilever is pinned to the substrate [21][23][22]. N_{EC} and N_P are introduced as illustrated in the equation below:

$$N_{EC} = \frac{2Eh^2t^3}{9\gamma_l \cos\theta_c l^4 (1 + \frac{t}{w})} \qquad (5)$$

$$N_P = \frac{3Eh^2t^3}{8\gamma_s l^4} \qquad (6)$$

where E is the Elastic (Young) modulus of a cantilever, γ_l is the liquid surface tension, θ_c is the

liquid-air contact angle, l is the cantilever length, t is the thickness of the cantilever, w is the width of the cantilever, h is the space between a cantilever and its substrate and γ_s is the solid surface tension.

To avoid stiction, we need to find the critical cantilever's length, i.e. the maximum length after which the cantilever is pinned to the surface. This critical length is called detachment length. When N_{EC} and N_P are equal to one, the cantilever length reaches the detachment length [22].

When

$$N_{EC} = 1 \rightarrow l = \left(\frac{2E}{9\gamma_l \cos\theta_c}\right)^{1/4} \left(\frac{h^2t^3}{1+t/w}\right)^{1/4} = L_d \qquad (7)$$

and

$$N_P = 1 \rightarrow l = \left(\frac{3E}{8\gamma_s}\right)^{1/4} (h^2t^3)^{1/4} = L_d \qquad (8)$$

$\left(\frac{h^2t^3}{1+t/w}\right)^{1/4}$ and $(h^2t^3)^{1/4}$ depend on the characteristic of cantilevers. By plotting the observed value of L_d as a function of $\left(\frac{h^2t^3}{1+t/w}\right)^{1/4}$ and $(h^2t^3)^{1/4}$, we are able to find the value of $|\gamma_l \cos\theta_c|$ and γ_s.

In addition, in the work that has been done by C. H. Mastrangelo and C. H. Hsu, they tried to release cantilevers in various lengths, gaps and widths with Polysilicon layer as a structural layer. To release these structures they used HF so the surface would be hydrophobic. The rinse liquid was water. They plotted the detachment length of cantilevers beams for hydrophobic samples as a function of the parameters $\left(\frac{h^2t^3}{1+t/w}\right)^{1/4}$ and $(h^2t^3)^{1/4}$. Figure 1.13 shows the result.

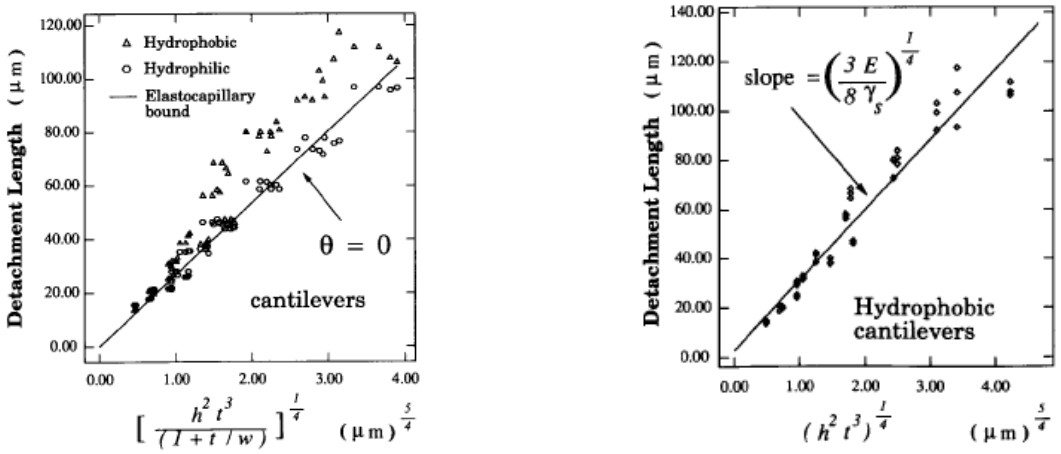

(a) (b)

Figure 1. 12 plot of the detachment length, L_d, a) versus $\left(\frac{h^2t^3}{1+t/w}\right)^{1/4}$ and b) versus $(h^2t^3)^{1/4}$ [23].

Both plots prove that the equation works perfectly when the last liquid during the drying process is water. By plotting the detachment length versus $\left(\frac{h^2t^3}{1+t/w}\right)^{1/4}$ and $(h^2t^3)^{1/4}$ the slope of the plot introduces the value of $\left(\frac{2E}{9\gamma_l \cos\theta_c}\right)^{1/4}$ and $\left(\frac{3E}{8\gamma_s}\right)^{1/4}$. Hence the value of $|\gamma_l \cos\theta_c|$ and γ_s from the slope is extracted. Fitted γ_s values of 100 ± 60 mJm^{-2} was found for hydrophobic samples [23].

In the other work, done by O. Raccurt *et al*. they did exactly the same process but this time they rinsed cantilevers in three different liquids, DI Water, IPA, and Pentane. When the last liquid for rinsing was water, their plot was fitted with the theoretical equation. Furthermore, for IPA and Pentane, the slope of the plot increased. Therefore, the value of $(\gamma_l \cos\theta)$ decreased as was predicted. Figure 1.14 shows their result for three different liquids (Water, IPA and Pentane).

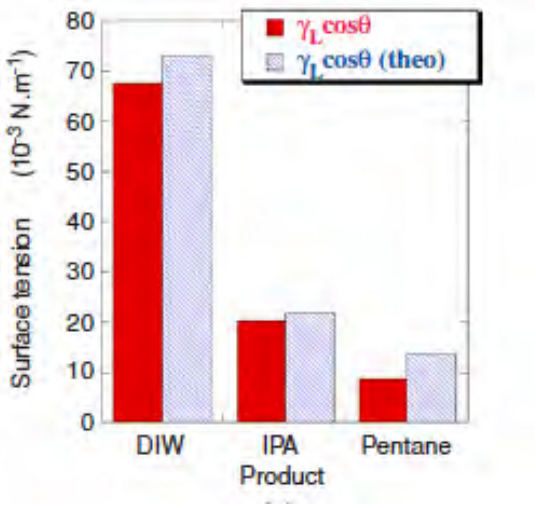

Figure 1. 13 Experimental liquid surface tension γ_l, calculated for DI Water, IPA and Pentane in comparison with the theoretical liquid surface tension [22]

However, theoretically the value of the γ_s has to be constant for various liquids. Because according to the equation 6, N_p does not affected by changing the rinsed liquid.

Their experimental result shows that the slope of the plot is different for various liquids. Hence, the value of γ_s changes for different liquids. The measurement result from experiments for γ_s is shown and compared in the Figure 1.15.

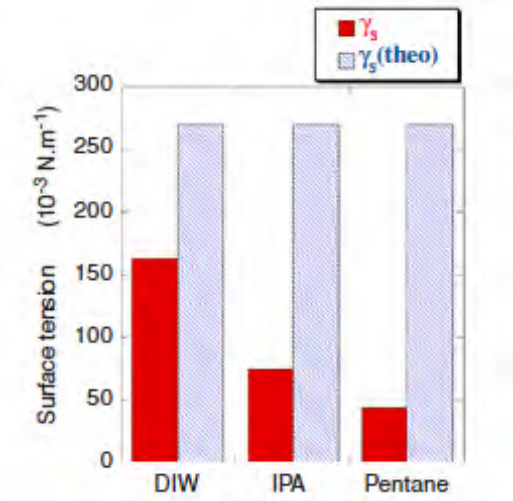

Figure 1. 14 Experimental solid surface tension γ_s, calculated for DI Water, IPA and Pentane in comparison with the theoretical solid surface tension [22]

We have to mention that all experimental results have been done on pure liquid. However, in the industrial environment, it is impossible to use pure IPA for drying process and to the best of

our knowledge, no experimental works involving rinse in the mixture of water and IPA has been conducted. To investigate the stiction when the last liquid during the drying sequence is the mixture of water and IPA, we need to know the liquid surface tension of mixture in different concentration of IPA. The next section is dedicated to this discussion.

1.9 - Liquid surface tension of water + IPA

For pure water and pure IPA, the value of γ_l is specified. However the surface tension of aqueous solution is variable and strongly depends on the concentration of solute and the temperature [24]. The table 1.2 shows the surface tension of Water + 2-Propanol (IPA) with various concentration for various densities that has been done in two different works:

Table 1. 2 Experimental and theoretical measured surface tension of the mixture of water + 2-propanol in various densities [24].

		$\sigma/(\mathrm{mN \cdot m^{-1}})$ at $t/°C$						
mass %	x_1	20	25	30	35	40	45	50
0	0.000	72.75	72.01	71.21	70.42	69.52	68.84	67.92
5	0.016	50.32	49.58	48.88	48.16	47.37	46.66	45.82
10	0.032	41.21	40.42	39.73	39.06	38.43	37.78	37.04
15	0.050	35.27	34.63	34.01	33.38	32.76	32.13	31.51
20	0.070	31.16	30.57	29.98	29.37	28.79	28.18	27.59
25	0.091	28.88	28.28	27.71	27.14	26.58	26.04	25.47
30	0.114	27.38	26.82	26.26	25.73	25.18	24.66	24.11
40	0.167	25.81	25.27	24.74	24.23	23.72	23.21	22.69
50	0.231	24.78	24.26	23.76	23.27	22.78	22.29	21.81
60	0.310	24.05	23.51	22.97	22.54	22.03	21.52	21.01
70	0.412	23.17	22.68	22.18	21.71	21.22	20.76	20.28
80	0.545	22.62	22.14	21.66	21.18	20.71	20.23	19.78
90	0.730	22.21	21.69	21.18	20.66	20.16	19.74	19.23
100	1.000	21.74	21.22	20.72	20.23	19.71	19.21	18.69

This table shows that by adding just 5% IPA in water, the surface tension of water reduces from 72 mJm^{-2} to 50 mJm^{-2} at 25°C. This is the main reason of using IPA during the rinse time to reduce the surface tension of water.

By spraying IPA at the surface of water, IPA reduces the surface tension of water to ease the separation of water from the surface of solid. Work of adhesion is an important quantity, which represents the work necessary to separate a drop from the solid surface [25][26]. If the contact

angle between drop and solid has finite value, the equation below calculates the value of work of adhesion [25]:

$$W_{AB} = \gamma_l (1 + \cos\theta_c) \qquad (9)$$

where A represents the solid and B refers to the liquid. W_{AB} is Work of Adhesion, γ_l is the liquid surface tension and θ_c is the contact angle between the liquid and solid.

1.10 – Motivation

Marangoni style dryer (LuCID) is considered a novel drying technique among other drying methods and there is very limited number of publications about the effects of this device. There are some patents on improving the efficiency of this device; however, more study has to be done to enhance the effect of this device.

Moreover, the effect of IPA on stiction is very important in LuCID. Still a significant amount of research is needed to define the effect of IPA on stiction or other types of failure in MEMS that is caused by using IPA. It is necessary to realize the outcome of using IPA on both drying and stiction at the same time.

Finally, there is a possibility of numerous IPA injections in LuCID (up to 10 times). These injections are designed to produce different concentrations of IPA at the wafer's surface. This is a good opportunity to check different setups of the LuCID for different substrates or etchants. Extensive experimental work is required to find the best setup, with the consideration of number of IPA injections and resulting IPA concentration during the drying process.

1.11 – Problem Statement

In this work we have worked on LuCID machine to find out the effects of Marangoni style dryer on drying technique. To do this the following preparation was conducted:

- Proper structures fabricated on silicon wafer with the ability to trap sufficient amount of water were required to test the effect of IPA on drying. The weight of trapped water must be high enough to be detected using a balance with 0.00001 readability. The reliable accuracy of the balance is 0.05 mg. Fabricating a test wafer with this ability is necessary to be able to compare the effect of LuCID Dryer.

- Design of the test wafers to check the effect of IPA on stiction during the drying process is also required. Finding the best concentration of IPA on the surface of water to dry and eliminate watermarks is not enough. It is necessary to detect the best setup by observing the best drying result along with the lowest amount of stiction between structures.

- Finally, it is necessary to make sure that the dryer or IPA will not add any contaminants on the substrate.

To the best of our knowledge this is the first time that these elements have been evaluated in combination on any Marangoni style dryers.

1.12 – Organization of Chapters

Chapter 2 presents an overview on Marangoni style dryer (LuCID) and its properties. In addition, the performance of this device is explained in details in this chapter.

Chapter 3 illustrates the fabrication of micro ribbons test wafers and cantilevers test wafers. In addition, introduces some of the measurement tools that have been used during this work.

Chapter 4 describes the micro ribbons test wafers and the reason of designing these wafers.

Chapter 5 details the experiment, which has been done on micro ribbons test wafer to test the effect of IPA on stiction.

Chapter 6 explains the reason of designing cantilevers test wafers. Furthermore, cantilevers test wafers were used to test the effect of IPA on stiction.

Chapter 7 investigates the deflection, mechanical stability and adhesion of cantilevers. Our experimental result is compared with previous works.

Chapter 8 includes conclusion and possible future works.

Chapter 2 – Low Consumption IPA Dryer (LuCID)

2.1 – Aim of the chapter

This chapter describes the LuCID. The tank and the lid of LuCID Dryer, as well as all parameters that are important in each drying recipe and the different type of IPA injections are explained individually.

2.2 – Drying process in LuCID Dryer (Akrion-Systems)

Low Consumption IPA Dryer (LuCID) is designed for rinsing wafers in deionized water (DI Water) and drying in the same setup. The whole process of drying is controlled by the computer and can be incorporated into any programmed process recipe. Drying process in LuCID contains six steps.

1. Pre-cycle process to clean the inner tank before the drying process will begin.
2. Wafer is submerged in the inner tank, which is filled with water.
3. Water drains from the inner tank slowly (Slow Drain) and simultaneously IPA is injected into the tank from the lid.
4. Slow draining and IPA injection will finish at the time that all the water will be extracted from the inner tank. (At this step Marangoni style drying will finish)
5. Hot nitrogen will flow into the inner tank to evaporate the remained water on the wafer.
6. Wafer is taken out of the inner tank.

In the following sections, all steps are described in details.

2.2.1 – The drying process

Before the beginning of the drying process, LuCID will perform the pre-cycle process. In pre-cycle time, the inner tank is filled with water before a wafer is delivered to the device. There is a tube that is responsible for water delivery before each cycle. The inner tank of LuCID is made of poly-vinylidene difluoride (PVDF). The capacity of the inner tank is ~50 liters. The device has an ability to inject some type of chemicals into the water. In this experiment no chemical liquid or gas has been injected into the water. After the inner tank is filled with the water, robot delivers the wafer and submerges it in the water (Fig 2.1-a). In the next step the tank lid closed and depending on the recipe we can have IPA injections before water drains down (Fig 2.1-b).

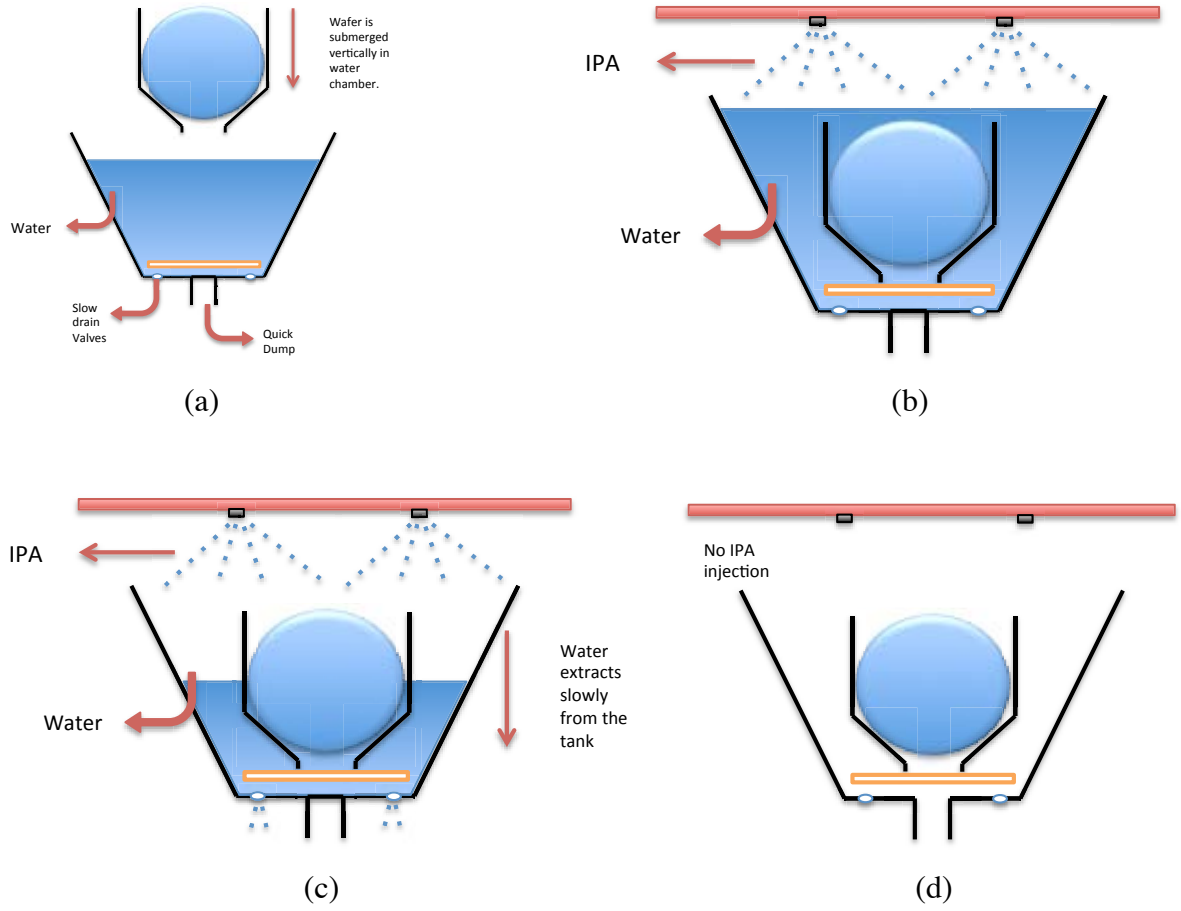

Figure 2. 1 The process of drying in LuCID: (a) Wafer is submerged vertically in the tank filled with water. (b) The tank lid closes and IPA is injected (IPA injection during the delay time). (c) The slow drain valves open and water goes out slowly. During this time, IPA is injected from the lid tank (IPA injection during the drain time). (d) After all water goes out from the tank, IPA injection will finish.

Then water begins to drain, slowly, and IPA is injected from the manifold that is placed in the tank lid (Fig 2.1-c). There are two types of holes beneath the inner tank to extract water from the inner tank:

1- Slow Drain
2- Quick Dump

Two valves are responsible for slow drain system. These valves are adjustable valves and are used to control the slow drain flow rate. The speed of draining is 1mm/sec and with changing the valves' setup we are able to increase or decrease this rate. For 200 mm wafer the drain time has to be around 4 minutes and 20 seconds. It means that it takes 200 seconds for the water to drain the equivalent of the distance from the wafer's top to bottom edges. Plus 30 seconds are needed to clear from the tank's top to top of the wafer and 30 seconds from wafer's bottom to the tank's bottom. The whole process takes 5 minutes and 20 seconds. Slow drain system is used during every drying sequence. During the slow drain time, IPA is being injected.

The other type of draining is a quick dump. Two large holes at the base of the inner tank are responsible for quick dump. When each drying sequence is finished, wafer is delivered out of LuCID and the inner tank again is filled with water. Then the water extracts from the inner tank very fast by using the quick dump holes. This process is designed to clean and prepare the inner tank for the next use.

2.2.2 – IPA Injection manifold

After a wafer is placed in the inner tank, the lid is closed. As water starts draining, simultaneously, the IPA injection occurs. IPA injection manifold is located in the lid of LuCID Dryer. The injection system comprises vaporizing tubes and a spray bar. Figure 2.1 shows the injection manifold inside the tank's lid. IPA flows inside the tube with the pressure of nitrogen gas and passes through the porous material. This porous material creates IPA vapor. Then, IPA is delivered to a spray bar at the center of the lid tank and is sprayed evenly into the inner tank.

Figure 2. 2 The injection manifold of LuCID Dryer and direction of IPA flow. The blue arrow shows the path that liquid IPA must pass to spray into the tank.

Up to ten IPA injections can happen during each drying process. In the device's default recipe (standard recipe) four injections occur during each drying process. The first injection begins exactly at the beginning of the slow drain time (the drain time) and other injections continue evenly till the end of the drain time. This type of injection is called injection during the drain time.

We should note that each IPA injection takes 10 seconds. However, after IPA injection, the vaporized IPA needs a time to reach from the tank's lid to the surface of the water. This timing is called Low Flow Time. Low flow time indicates the duration between IPA injections when the cloud of vapor IPA is purged into the inner tank with a low flow of nitrogen. Also, during this time, the device has a sufficient time to recharge IPA for the next injection.

slow drain delay time	10
1st IPA inject time	0:10
1st IPA low flow time	1:00
2nd IPA inject time	0:10
2nd IPA low flow time	1:00
3rd IPA inject time	0:10
3rd IPA low flow time	1:00
4th IPA inject time	0:10
4th IPA low flow time	1:00
:	0:00
:	0:00
:	0:00
10th IPA inject time	0:00
10th IPA low flow time	0:00

Figure 2. 3 The figure shows the timing of each IPA injection for Standard Recipe. In standard recipe IPA is injected four times during the drain time. Each injection takes ten seconds. After each injection for one minute there is no IPA injection. During this time the cloud IPA flows down inside the inner tank.

In Standard recipe for the 1st IPA injection time; IPA is injected for 10 seconds. Then there is a low flow time when no injection occurs for 1 minute. During the low flow time the cloud of vapor IPA flows down inside the inner tank and covers the air-water interface. After that, the 2nd injection occurs and all steps repeat again till the fourth low flow time. After the 4th low flow time the slow drain time is finished and no more IPA is injected.

IPA injection also can happen during a delay time. Delay time delays the opening of the slow drain valve and water does not go down. If the delay time is set to 0, the slow drain valve opens and the IPA injection begins simultaneously and the drying process begins. If delay time is programmed to number of seconds higher than zero, it delays the drain time, and IPA injection begins. It means that the slow drain valve stays closed until the delay time expires. This delay allows an IPA vapor to build a sufficient density and fills the volume above the DI water in the inner tank. The delay time can be set up to maximum of 99 seconds.

slow drain delay time	35
1st IPA inject time	0:10
1st IPA low flow time	0:25
2nd IPA inject time	0:10
2nd IPA low flow time	1:00
3rd IPA inject time	0:10
3rd IPA low flow time	1:00
4th IPA inject time	0:10
4th IPA low flow time	1:00
5th IPA inject time	0:10
5th IPA low flow time	1:00
:	0:00
:	0:00
:	0:00
10th IPA inject time	0:00
10th IPA low flow time	0:00

(a) 1-Time Injection

slow drain delay time	75
1st IPA inject time	0:10
1st IPA low flow time	0:25
2nd IPA inject time	0:10
2nd IPA low flow time	0:25
3rd IPA inject time	0:10
3rd IPA low flow time	1:00
4th IPA inject time	0:10
4th IPA low flow time	1:00
5th IPA inject time	0:10
5th IPA low flow time	1:00
6th IPA inject time	0:10
6th IPA low flow time	1:00
:	0:00
:	0:00
:	0:00
10th IPA inject time	0:00
10th IPA low flow time	0:00

(b) 2-Times Injection

slow drain delay time	99
1st IPA inject time	0:10
1st IPA low flow time	0:25
2nd IPA inject time	0:10
2nd IPA low flow time	0:25
3rd IPA inject time	0:10
3rd IPA low flow time	0:19
4th IPA inject time	0:10
4th IPA low flow time	1:00
5th IPA inject time	0:10
5th IPA low flow time	1:00
6th IPA inject time	0:10
6th IPA low flow time	1:00
7th IPA inject time	0:10
7th IPA low flow time	1:00
:	0:00
:	0:00
:	0:00
10th IPA inject time	0:00
10th IPA low flow time	0:00

(c) 3-Times Injection

Figure 2. 4 The figure shows the different type of setup for different recipe. The first row in each column indicates the delay time. The delay time delays the drain time, and let to have IPA injection. This delay allows IPA to make a sufficient density at the interface of water-air a) Timing of each parameter for the recipe with one time injection during delay time and 4times injection during drain time. b) Timing of each parameter for the recipe with 2times injection during delay time and 4times injection during drain time. c) Timing of each parameter for the recipe with 3times injection during delay time and 4times injection during drain time.

Figure 2.3 shows three different recipes. In these recipes IPA is injected during delay time. The figure illustrates recipes with 1, 2, and 3 times IPA injection during the delay time. In this study, we dedicated significant amount of work to these three recipes and compared the results to the standard recipe. In all recipes after IPA injection finished, the quick dump valve opens to remove the remained DI water in the inner tank.

After the Marangoni style drying (IPA injection), a high flow of hot ionized nitrogen gas is injected into the tank for 15 minutes. This timing is adjustable and we can vary this time by the recipe. The nitrogen gas is delivered to the N2 spray bar that is shown in figure 2.1. The nitrogen gas is heated to 145 ℃ (125 ℃ on the wafer surface) to evaporate the remaining water and is ionized to neutralize possible static charges on and around wafers. Heated nitrogen process takes 15 minutes in our recipe.

The size of the inner tank is 417mm in length × 241mm in width. In each injection 2.5 ml of IPA is injected into the tank. The table below shows the chemical properties of IPA at 25° C.

Table 2. 1 Chemical properties of IPA. (The value of Diffusion Coefficient at 25° **C**) [27].

Properties	Molar Mass	Density	Diffusion Coefficient
IPA	60.1 g/mol	0.786 g/cm^3	0.0959 (cm^2/s)

In each injection 0.03257mol of IPA is injected, which is equal to 1.97×10^{22} molecule of IPA. The IPA spray bar is designed to spray IPA evenly on the surface of water. By measuring the surface area of the inner tank we are able to find the number of IPA's molecule per square centimeter at the surface of water after each injection. The surface area of inner tank is 1004.97cm^2. Therefore, after each injection: $1.96\times10^{19}\ molecule/cm^2$ IPA covers the surface of water.

Chapter 3 – Test wafers Fabrication and Measurement tools

3.1 – Aim of the chapter

In this chapter the fabrication of test wafers is first described, then detailed description of the metrology equipment used in our work is presented. To determine the height of released structures, Nanometrics device (will described later on) was used in this research. Film thickness measurements were conducted on N&K Olympian tool (will described later on). Visible range automated inspection tool, Rudolph (will described later on), was used to detect and count the number of defects in the test wafers. Finally, to analyse the surface chemistry of wafers, X-Ray Photoelectron Spectroscopy (XPS) was used.

3.2 – Test Wafer and Its Fabrication

For this study two types of test wafers were fabricated:

1- Micro-Ribbons Wafers

2- Cantilevers Wafers

3.2.1 – Fabrication of Test Wafer

All test wafers were fabricated on silicon wafers with 200mm diameter. Fig 3.1 shows the fabrication process. To fabricate the test wafers, first of all, a uniform layer of PECVD oxide was deposited on p-type silicon (100) (Fig 3.1-b). Then the oxide layer was annealed at 1100℃ temperature to make dense PECVD oxide layer (Fig 3.1-c). The thickness of oxide layer after annealing is $1.5\mu m$. This layer is a sacrificial layer. In-Situ Doped Polysilicon (ISDP) and Low-Stress Nitride (LSN) layers are popular structural layers for the fabrication of MEMS structures. For this reason, we decided to use ISDP and LSN as a structural layer on our test wafers. ISDP

film was deposited on six wafers, and LSN film was deposited on three wafers. The thickness of the ISDP layer was 2 microns, and the thickness of LSN layer was 435 nm (Fig 3.1-d).

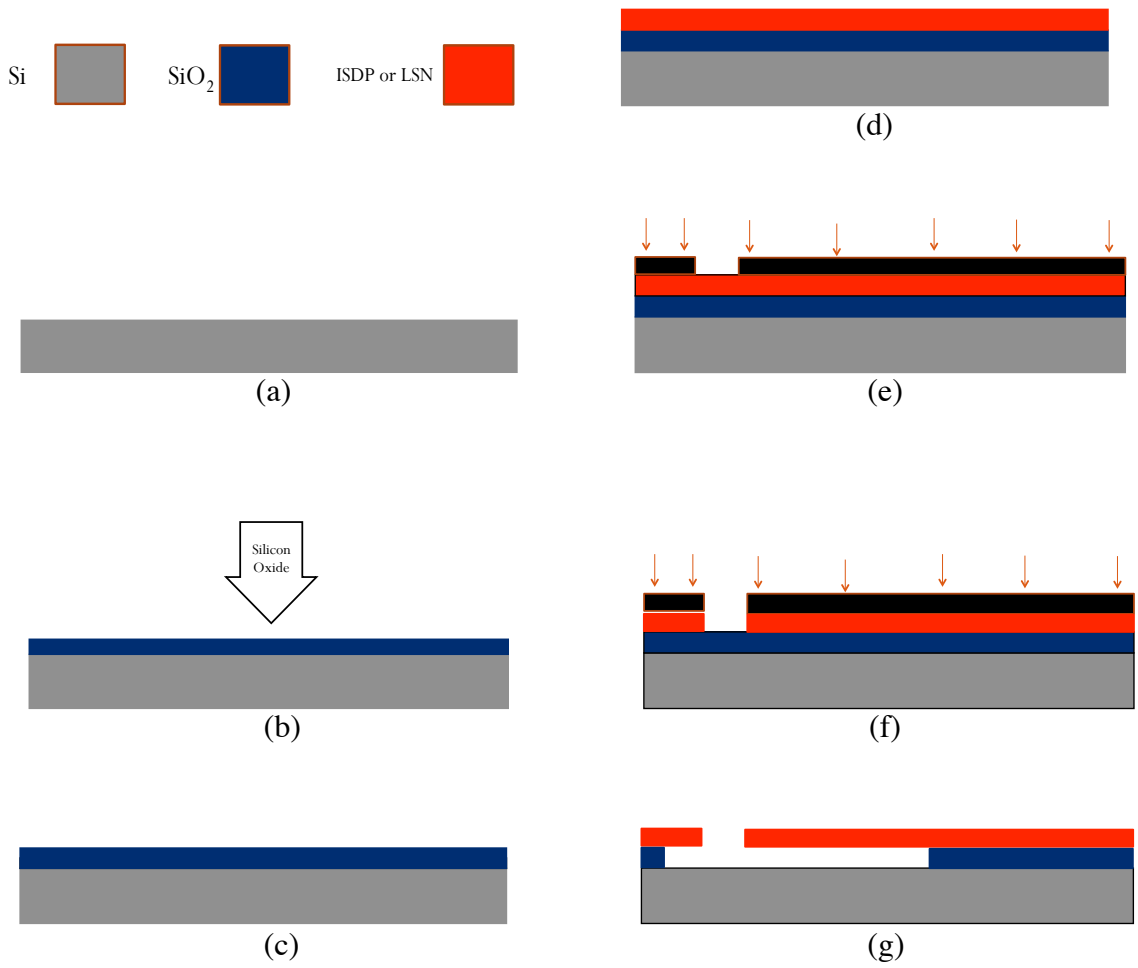

Figure 3. 1 Simplified fabrication process of cantilevers (a) Initial Silicon Substrate. (b) Deposition Plasma enhanced chemical vapour deposition (PECVD). (c) Annealing in 1100℃ in $\boldsymbol{O_2}$ and grow an oxide layer. (d) Deposition of ISDP or LSN layer. (e) Mask alignment and using UV light to pattern structures. (f) Bombarding wafers with heavy ions (etching the surface layer by RIE). (g) Etch the sacrificial layer by DHF (10:1) or BOE.

After deposition of the structural layer, the next step was the lithography. In this step, wafers were coated with positive photoresist and then exposed to i-line radiation on 5x stepper, ASML (Fig 3.1-e). After inspection of each wafer with a microscope, wafers were transferred to etch the structural layer with dry etching (Fig 3.1-f). After that, remaining photoresist must be removed. One of the techniques is wet resist stripping. In this technique, the remained photoresist is etched

by submerging the wafer in acetone. Wet resist striping cannot clean the photoresist completely, and acetone leaves residue on the surface of a wafer. Plasma stripping is more prevalent in the industry. Plasma striping is dry technique, and normally a specific device is designed for this purpose. As a result, for our test wafers we used the oxygen plasma stripping technique using ULVAC oxygen plasma tool.

For Micro-Ribbons Wafers another inspection followed, to confirm pattern's conformity. The Figure bellow shows the micro-sized ribbons after lithography. The width of each ribbon is 3.2micron with the gap of 0.5um

Figure 3.2 The micro ribbons after lithography. These ribbons are not released yet.

The mask Cantilevers Test Wafer is special. Fig. 3.3 shows the layout of mask for these wafers. The mask contains cantilevers with widths of 1.5, 2.5 and 3.5 microns and various lengths from 30 to 600 microns. These cantilevers are suitable to test the stiction after wet etching and drying process.

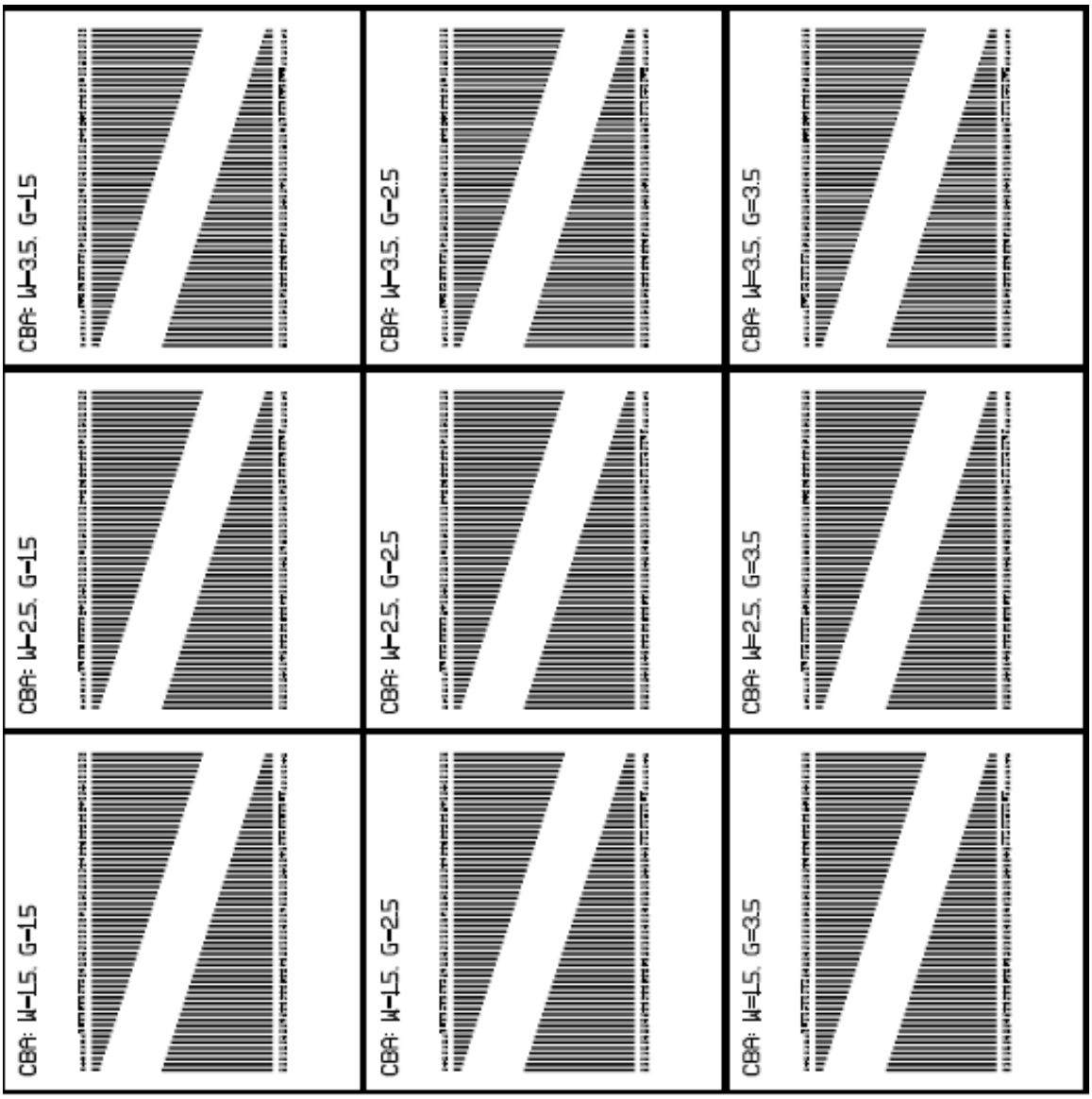

Figure 3. 3 The mask of Cantilever-wafer. This test wafer contains cantilevers with widths of 1.5, 2.5 and 3.5 microns and various lengths from 30 to 600 microns. Each smaller die contains two rows of cantilevers.

Moreover, all wafers were inspected with an optical microscope. The last step in the fabrication of these wafers is wet etching to release the structures (Fig 4.1-g). However, for Micro-Ribbons Wafer because the ribbons are thin, it is really hard to confirm if the ribbons were released completely or not after wet etching of sacrificial layer. To check all ribbons were released completely, some cantilevers were designed in the mask of this wafer. These cantilevers

are placed beside each row of ribbons in each die. The width of these cantilevers is from 3.5 microns to 6.5 microns. Fig. 3.4 and 3.5 shows these cantilevers. The purpose of these cantilevers is to make sure that the ribbons are released. After etching and releasing the ribbons, we observed the deflection on cantilevers with the width of 5 microns, using optical microscope. Since the cantilevers with 5 microns width were etched and released completely, then it is safe to assume that all sacrificial TEOS was removed and the ribbons with width of 3.2 micron were released properly.

Figure 3.4 Cantilevers with widths between 3.5 and 6.5 microns are shown in this figure to check that ribbons released completely. Since the ribbons in Micro-Ribbons Wafer are thin, it was difficult to check them with a microscope. So, if cantilever till 5 microns were etched perfectly, then we can be sure that the ribbons had been etched completely.

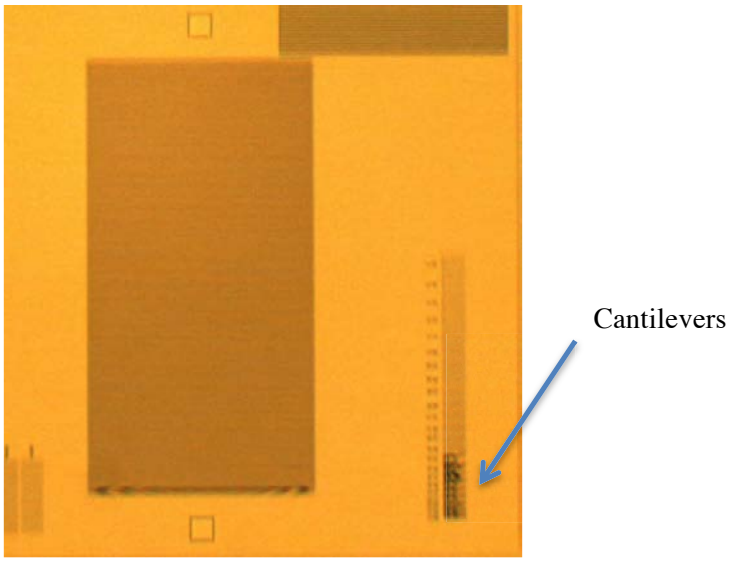

Figure 3.5 The figure shows the Released Micro-Ribbons Wafer. This wafer has the ability to trap water beneath its ribbons and by this capability we can test the effect of IPA on drying.

For Cantilevers wafers the main purpose for the fabrication of these test wafers is to test the stiction in cantilevers with different lengths and widths. For this purpose, the engineering mask has been used and for the structural layer ISDP was selected. Three Wafers were released with DHF, and one wafer was released with BOE. These two chemicals are the most common etchant for a sacrificial oxide layer. It is estimated that the cantilevers with the length below 150 microns are released with no stiction but by increasing the length of cantilevers, the probability of stiction increases. Figure 3.6 Shows cantilevers with the small length from 30 to 90 microns. Most of the cantilevers with these dimensions are released without any stiction.

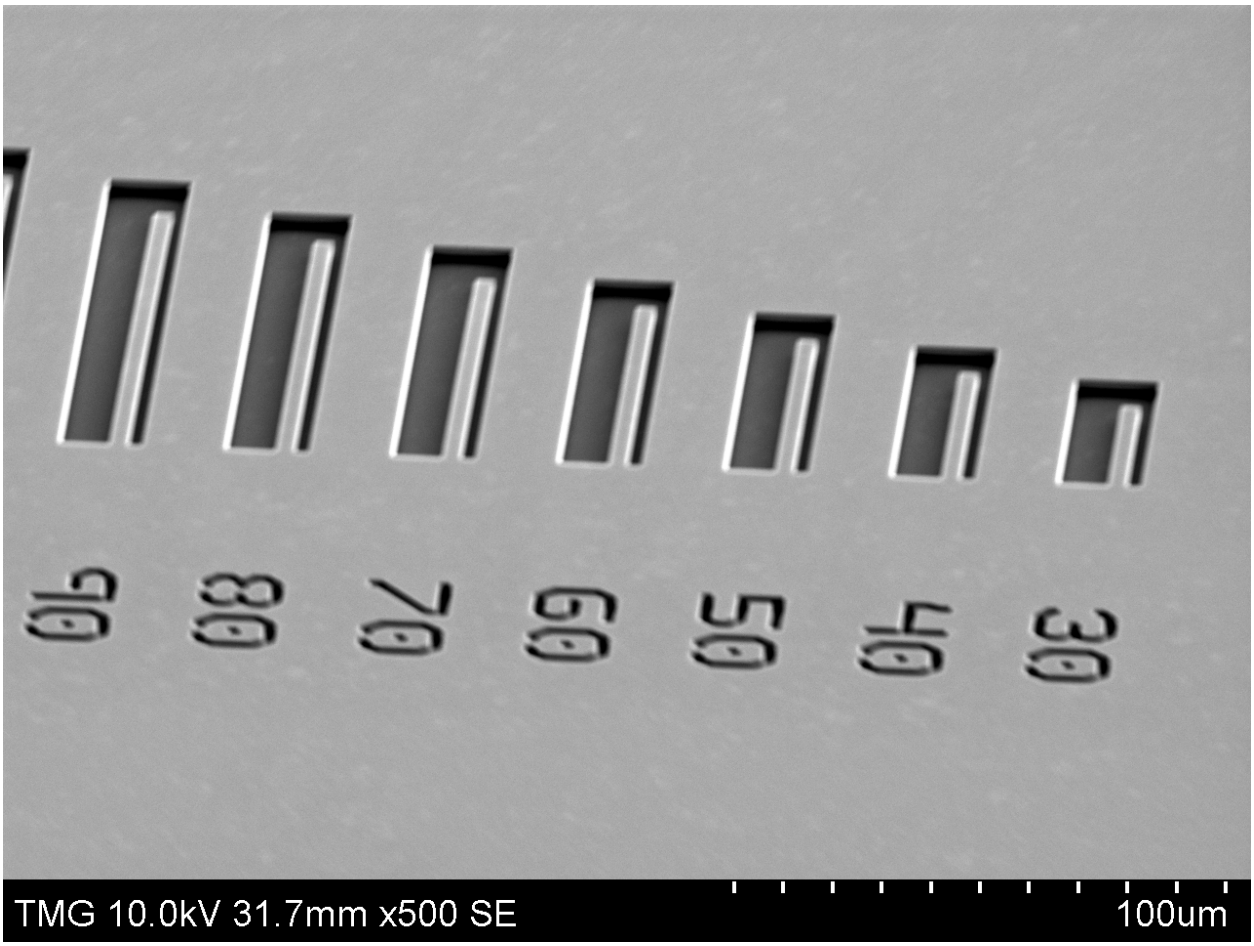

Figure 3.6 The SEM image of released cantilevers with length between 30 to 90 microns. These Cantilevers are suitable to test the effect of IPA on stiction by trying different drying recipes.

Figure 3.7 shows the result for the case that the length of cantilevers is bigger than 150 microns. In this figure, the length is between 150 and 200 microns. As it shown in the figure, all cantilevers stick to the bottom or to the side.

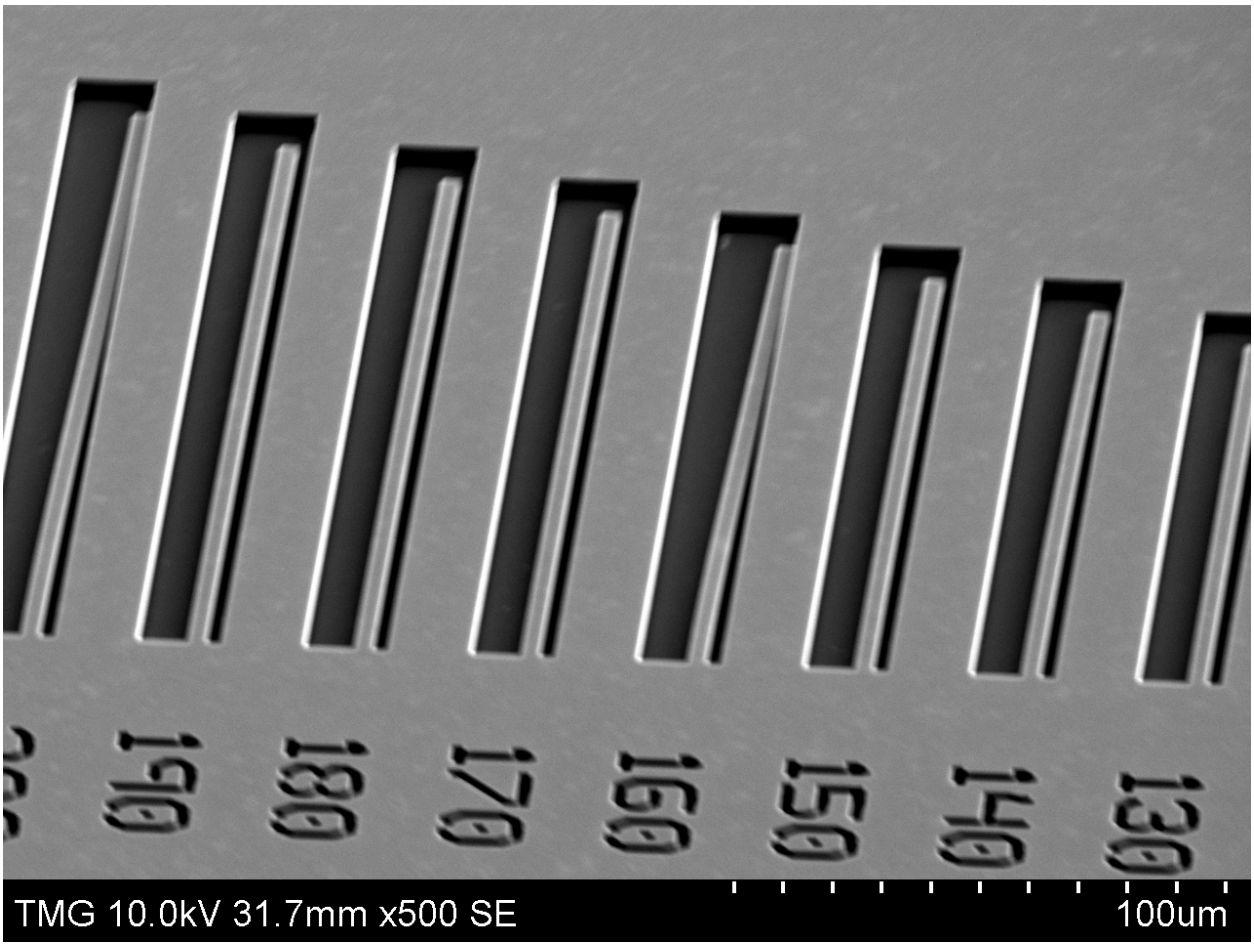

Figure 3.7 The SEM image of released cantilevers with length between 130 to 200 microns. Mostly all cantilevers with lengths higher than 150 microns, stick to the bottom or to the sides.

The process above was the brief description of the fabrication of test wafers. Three wafers with ISDP layer as a structural layer were etched with Buffered Oxide Etch (BOE) to test the effect of IPA on drying.

3.3 – Measurement Devices

3.3.1 – Nanometrics

Nanometrics is a 3D scanner device for pattern recognition and providing multiple Critical Dimensions (CD) on one measurement. This tool is able to detect repeatable critical dimensions

of the most challenging within – die product structures, such as the etch depth of microstructures on the surface of wafer [28].

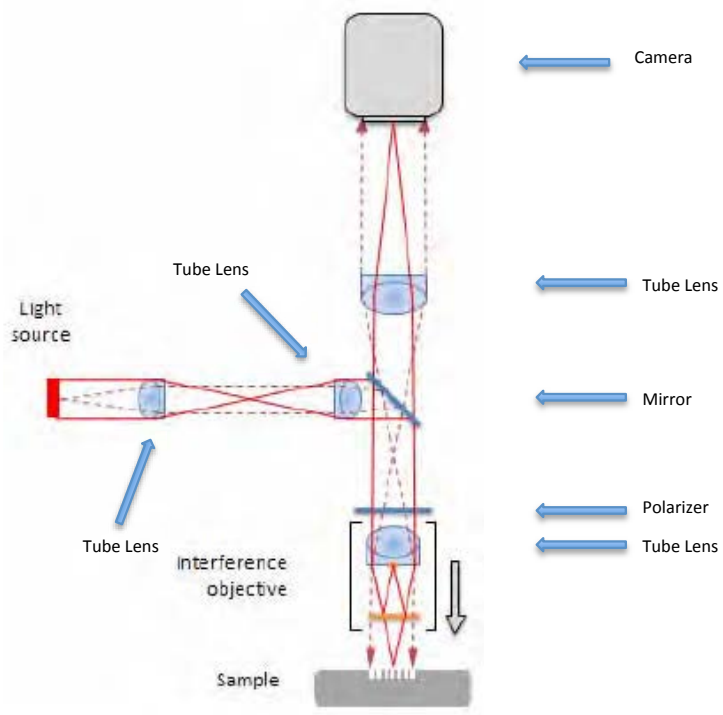

Figure 3.8 The figure shows the schematic of Nanometrics device. White light emits from the source. Mirrors and tube lenses lead the light into the surface of the sample. The polarizer increases the sensitivity of measured etch depth. Camera captures the reflected lights, and send the records to the computer to scan the position of the reflected light [29].

Normally, in this device, a visible wavelength emitted on the wafer surface and a camera captures the reflected light and send the records to the computer to scan the position of the reflected light [29]. A linearly polarized light is used to increase the sensitivity of the device. To measure the depth of any structure by computer, domain and frequency of the reflected light is analysed [29]. The software uses the numerical modeling to measure the diffraction of electromagnetic waves on periodic grating [30]. Among all kinds of modeling, Rigorous Coupled Wave Analysis (RCWA) method is the method that is used in Nanometrics device. RCWA modeling is widely used for space periodic parts to analyse the depth and height of structure.

As mentioned before in Nanometrics white light is used to measure the height of structures on the wafer surface. Figure below shows that the white light is emitted on the surface with periodic parts with 200 nm pitches. The left figure shows the two-dimension scan of the structure. The software calculates the intensity of each scan position z (vertical axis) and at each object-space pixel position x (horizontal axis) and extracts the height of structure along the x axis [30].

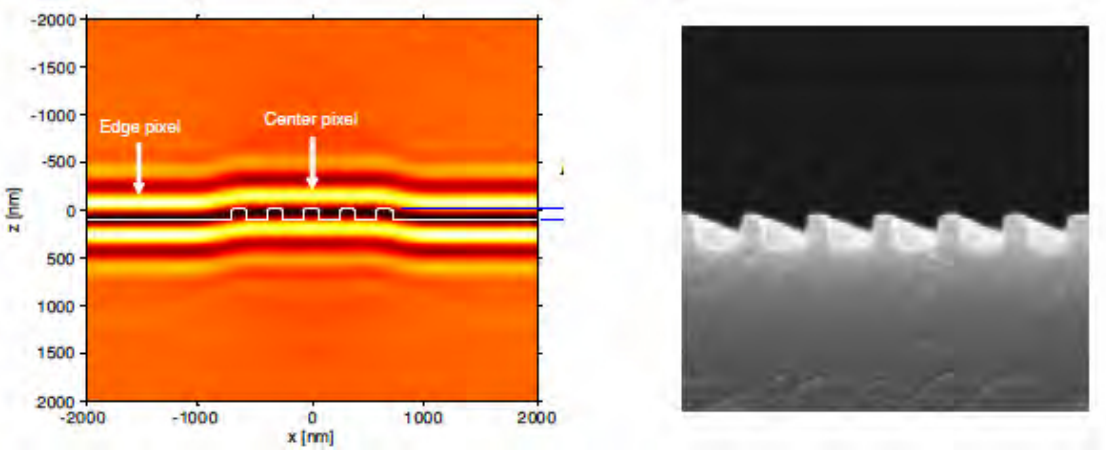

Figure 3. 9 Left figure is an example of RCWA calculation by scanning the structure. Computer scans the intensity of reflected light and compares the difference of intensity and calculates the differences of height between edge and canter pixel along x direction. Right figure illustrates the similar structure that captured by electron microscope image [29].

In this work, Nanometrics was used to define the height of released micro ribbons. Depending on a measurement recipe given to Nanometrics, the device can detect different amount of points inside the test wafer. In this work Nanometrics measured 17 points in each 200 mm diameter test wafer. Figure 3.3 shows the points that Nanometrics measures in this work. Nanometrics measures the height of the middle of each ribbon in comparison with the surface of the wafer. If the height of ribbon is higher than the height of surface the measurement is positive and if the height of the ribbon is lower than the surface, Nanometrics gives the negative result.

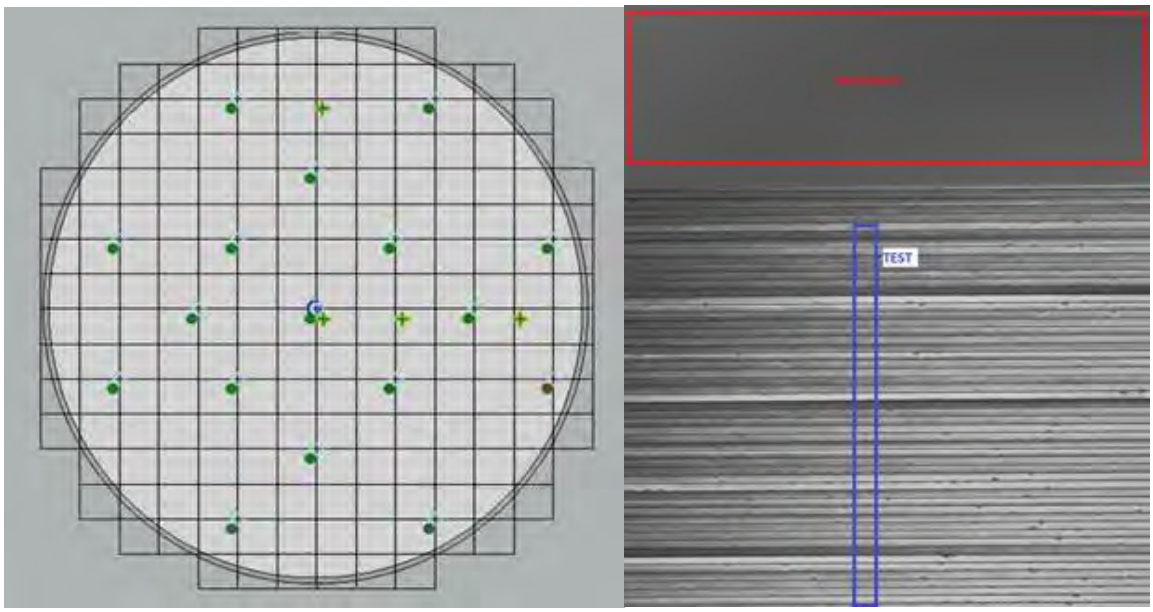

(a) (b)

Figure 3. 10 The figure shows Nanometrics measurement for our test wafers. a) The green points illustrate 17 spots that Nanometrics measured in each test wafer. b) The picture shows the released ribbons. Nanometrics measures the height of surface (red rectangular) and considers it as zero. The blue rectangular shows the exact position that Nanometrics measures the height of released ribbons. Nanometrics compare the height of blue rectangular with the height of the surface.

3.3.2 – N & K

This device is used to measure the thickness of thin films. The Spectroscopic Reflectometry is the method that is used in this device for the metrology. N & K emits light and gets the data from the wavelength of the reflected light. Different wavelengths are used for different films. For example for organic films and metals, UV is used for measurement, or for polymer layers Far-Infrared (FIR) wavelength is used [31]. The difference of the reflected wavelength between the thin film and the main substrate is the key point to measure the film thickness in this device [32]. Then, a computer analyses the data and based on the model extrapolates the thickness of the film [33]. During the measurement, N&K has no physical contact with a surface of a wafer; hence, there is no risk of destroying the thin film. It is understood that the photo-sensitive films will be affected. This device can detect the thickness between 190 nanometers and 15 micrometers [6].

Figure 3. 11 Thin film metrology tool (N & K) at C2MI Company [31].

The main usage of this device in this study is to find the etch rate of each material in various etchant for wet etching. For example, to find the etch rate of silicon oxide in HF, single layer of oxide was grown on the surface of the silicon. Then, using N&K, the thickness of the oxide layer was measured. Furthermore, the wafer was submerged in HF tank for 10 minutes. Again the etched wafer is placed in N&K device and the thickness of the oxide layer is measured after etching. The difference of the thickness with respect to the time of etching, gives us the etch rate of oxide in HF.

3.3.3 – Visible Range Automated Inspection (Rudolph)

Rudolph is the automated inspection device, which allows counting the defects on the surface of 200 mm wafer. Rudolph is capable of conducting the inspection on various types of wafers, e.g. silicon wafer, glass wafer, etc. [34]. The resolution of the device is between 0.05 and 10 microns. Rudolph is used to detect any type of defects on wafers and also it is very useful to count the number of contaminants on the surface of wafers.

Figure 3. 12 Rudolph for defect inspection at C2MI Company [34].

The main technology that is used in Rudolph to scan the wafer is Laser triangulation technology [35]. The technology is a line scan laser with the ability to collect hundreds of 3D data points along one scan line in a fraction of a second [40].

In this work, Rudolph was used to detect and count numbers of defects on the test wafers with cantilevers. Rudolph scans the wafer with unreleased cantilevers and assumes that this scan shows the cantilevers with no defects, creating a golden die. Then after releasing the cantilevers, the test wafers were scanned again by the Rudolph. The device compares the released scanned picture with the picture of unreleased cantilevers. Rudolph considers any differences between these two pictures as a defect and counts the number of defects during the inspection. In our recipe the accuracy of Rudolph was 1 µm.

3.3.4 – X-Ray Photoelectron Spectroscopy (XPS)

X-Ray Photoelectron Spectroscopy (XPS) is used to analyse the surface chemistry of a material. In this device the X-Ray beam is exposed on the sample's surface and, simultaneously, the device measures the kinetic energy and the number of electrons that escape from the surface [36]. There is a photoelectron spectrum in the device to count the number of ejected electrons. By measuring the energy and intensity of the photoelectrons, XPS is able to detect the atoms,

which exist at the surface of a sample. To have more accurate result, all samples must be kept in high vacuum chamber inside XPS device. Figure below shows the schematic of this process.

All the processes in this device could be summed up to the equation below:

$$E_{binding} = E_{X-ray} - E_{kinetic} - W_f \quad (1)$$

where $E_{binding}$ is the binding energy of the electron, $E_{X\text{-}ray}$ is the energy of the X-ray photons, $E_{kinetic}$ is the kinetic energy of the electron as measured by the analyzer, and W_f is the work function dependent on both the spectrometer and the material [37]. As it was defined in [38], the work function is an adjustable instrumental correction factor that accounts for the few eV of kinetic energy given up by the photoelectron as it becomes absorbed by the instrument's detector. The energy of the X-Ray is specific. XPS measures the kinetic energy of the emitted electron in the detector, and then calculates the binding energy. By finding the value of the binding energy, XPS is able to detect the atoms at the surface.

The device has the ability to focus and scan X-Ray beam. The X-Ray spot size can change from 7 to 300 microns [39]. XPS can detect 3 atomic layers at the surface (1 to 10 nm). In our study we used XPS to detect the atoms exist at the surface of our samples.

Chapter 4 – The effect of IPA on drying

4.1 – Aim of the chapter

This chapter represents Micro-Ribbons Wafers as well as the structure of the dies. The effect of IPA in drying, the Marangoni style drying, and its comparison with other drying process were investigated in this chapter.

4.2 – The effect of IPA on drying

For this study it was required to have structures with ability to trap water in order to test the effect of IPA on drying. After several designs fabricated and tested on silicon wafer, micron size ribbons with cavities beneath them were found to be suitable for our experiments. These wafers that we refers to as Micro-Ribbons Wafers were described in the previous section.

The purpose of this experiment is to see the effect of IPA on drying. IPA is used in LuCID to decrease the surface tension of water to facilitate the water removal from the surface of the wafer as well as from the cavities under the ribbons, and also to create a Marangoni effect to dry the wafer properly. For this reason, we designed and fabricated wafers with micro size ribbons.

Figure 4. 1 Photo sample of Micro-Ribbons Wafer. The main purpose of this wafer is beneath these ribbons is a cavity to trap water. This capability gives us opportunity to test the effect of IPA on drying.

The mask of the wafer is designed for 200 millimeters diameter silicon wafer and includes ninety-six dies with ribbons in various lengths. However, the width of all ribbons in all dies is 3.2 μm. As is shown in Figure 4.1, in the middle of each die, there is a row of ribbons, with the 1.5 μm deep cavity beneath. These cavities are able to give us the opportunity to trap water. Furthermore, by comparing the mass of the wafer before and after drying the wafer with LuCID, we are able to see the effect of LuCID in drying.

The first experiment was to find the effect of IPA on drying in comparison in the complete drying process. For this reason, we put three wafers with micro ribbon structures, one at the time, using the recipe with no drying sequence. In this recipe, which is called Recipe 1, there is no injection of IPA in LuCID Dryer and no flow of hot nitrogen. The purpose of this recipe is to find the average mass of wafer without drying conditions. Here, the weight of wafer will be the highest amount possible. The result is shown in Table 4.1.

Table 4. 1 the weight of wafers with no drying sequences. In this test, there is no injection of IPA in LuCID Dryer, no flow of hot nitrogen and no vacuum dryer. The purpose of this test is to find the average mass of wafer without drying conditions.

Recipe 1			
	Wafer 1	Wafer 2	Wafer 3
Weight of wafer before Recipe 1 (gr)	53.31592	53.31588	53.31582
Weight of wafer after Recipe 1 (gr)	53.31738	53.31715	53.31713
Difference of the mass (mg)	1.46	1.27	1.31

For measuring the weight of wafers, it takes 5 minutes and 20 seconds to transfer each of them from the bench to the balance. Because of this delay, it is possible to have errors due to water evaporation during the transition time, but this is unavoidable. The average weight of these three wafers is 53.31722 gr, and this value is the average weight of wafers when there is no drying circle in wet etching. The average mass difference (before and after Recipe 1) is 1.35 mg that corresponds to the mass of the trapped water.

For the next step, we want to see the effect of complete drying sequences on drying wafers. As mentioned before, the full process of drying (Recipe 2) consists of the LuCID dryer with IPA injection, a hot flow of nitrogen for 15 minutes. For this step, we expect to have wafers with lower weight than Recipe 1 because there is a complete drying sequence.

Table 4.2 shows the result of the second test.

Table 4. 2 The weight of wafers after complete drying sequence. In this test, after the wafer is placed in a water container, the wafer was dried with injection of IPA and hot nitrogen flowed on the surface of wafer for 15 minutes and finally the wafers were placed in vacuum dry chamber.

Recipe 2			
	1	2	3
Weight of wafer before Recipe 2 (gr)	53.31592	53.31588	53.31582
Weight of wafer after Recipe 2 (gr)	53.31609	53.31591	53.31586
Difference of the mass (mg)	0.17	0.03	0.04

The average weights of wafers in the Recipe 2 is 53.31595 gr and is less than the weights of wafers in the Recipe 1, as was expected. The average mass difference (before and after Recipe 2) is 0.08 mg.

This experiment was the most important step of the entire research. Significant efforts were put to design and fabrication of the appropriate test wafer with ability to trap detectable amount of water.

In conclusion, this experiment shows that the average mass of wafers after using Recipe 2 is 1.27 mg less than mass of the ones after using Recipe 1. It means that these wafers can trap around 1.27 mg of water after using Recipe 1 in addition to the 0.08 mg of water that would be trapped anyway even if we use Recipe 2. The 1.27 mg difference corresponds to the effect of LuCID used in Recipe 2. Now we are able to find the effect of IPA injection (Marangoni style drying) and compare with the other steps of drying (hot flow of Nitrogen).

4.3 -The effect of IPA injection in drying

In this step, we want to know the effect of Marangoni style drying in comparison with the whole drying process. For this purpose, a new recipe (Recipe 3) has been tried. In this recipe, wafers were again placed in the rinse tank and after that, they were placed in LuCID. In this recipe, there is an injection of IPA inside LuCID, but there is no hot nitrogen flow. By comparing the result of this recipe with Recipe 2, we are able to determine the effect of IPA injection (Marangoni style drying) in drying cycle. As mentioned before, there are two different types of IPA injections in LuCID dryer. At first, we tried Recipe 3 by changing the number of injections just during the slow drain time. Table 4.3 shows the result of drying the wafer by increasing the number of injections during this time. It is important to notice that, in the standard recipe, for Marangoni style drying, LuCID injects IPA four times during the slow drain time and there is no injection during the delay time.

Table 4. 3 The weight of the wafer after just Marangoni style drying. There are IPA injections just during the drain time. (4 times injection is the standard recipe for LuCID dryer). The middle column shows the weight wafer after dry the wafer by increasing the number of injection during the drain time. The right column compares the weight of the wafer with the test with no drying sequences.

Number of Injection During the drain time	**Weight After Drying Cycle (gr)**	**Difference Compared to Averaged Wafer Mass without the Drying Cycle (mg)**
2 times injection	53.31718	-0.04
*4 times injection	53.31717	-0.05
6 times injection	53.31719	-0.07
8 times injection	53.31731	+0.09

Based on the information from Table 4.3 we may observe that the mass of wafer when there are IPA injections during the drain time is lower than the mass of wafer after no drying sequence. By increasing the number of injection during the drain time up to 8, the weight of wafer is lower than after the recipe with no drying cycle. However, in case of 8 times injections, the weight of wafer is increased compared to the cycle no drying. The reason for this unexpected weight increase might be due to the fact that, by increasing the number of injections during the drain time, more IPA sprays into the tank, and it causes increase in concentration of IPA on the surface of the wafer. Higher concentration of IPA cannot make a Marangoni effect on the surface of the water. For this reason, the weight of wafer is greater than the others.

In the next step, we are looking to check the effect of IPA in LuCID Dryer when there are both types of injections – during the delay time as well as during slow drain time.

Table 4.4 illustrates the summary of the tests comprising injections during both the delay time and the slow drain time. The last column in Table 3.4 compares the weight of wafers from tests with no drying sequence. We should state that the maximum number of IPA injection in LuCID Dryer cannot exceed ten (10). Based on the results illustrated in table 4.4, IPA injections during delay time have a notably better effect on drying. The best outcome happens, when we have

three times injection during delay time and 4 times injection during the slow drain time. Again similarly to the result from Table 4.3, by increasing the number of injection during the slow drain time the weight of the wafer is getting higher.

Table 4. 4 The weight of the wafer after just marangoni style drying. There are IPA injections both during the delay time and the drain time. The last column compares the weight of the wafer with the test with no drying sequences. It should be noted that the recipe with 3-times injection during the delay time and 4-times injection during the drain time gives the best result.

Number of Injection During Delay Time	Number of Injection During Drain time	Weight After Drying Cycle (gr)	Difference Compared to Averaged Wafer Mass without the Drying Cycle (mg)
1	4	53.31697	-0.25
2	4	53.31702	-0.20
3	4	53.31692	-0.30
1	8	53.31711	-0.11
3	7	53.31714	-0.08

4.4 – Result and discussion

First of all, this experiment confirms that IPA has an effect on drying. The complete cycle of drying is able to decrease 1.27 mg of the weight of wafer in comparison with no drying cycle (the experiment in section 4.2) and the Marangoni style drying is responsible of 0.3 mg of this reduction (in the best result), which is 23% in comparison with the complete drying sequence.

Second of all, when there are both types of injections, the influence of IPA on drying is more efficient. Table 4.4 shows that when there are injections of IPA during the delay time, IPA is more effective (more capable of making a Marangoni effect) in comparison with injections only during the slow drain time. By increasing the number of IPA injection the effect of IPA decreases and it evident that we need to search the best recipe for LuCID in the case of the

numbers of IPA injections. This means that for the Marangoni style drying we cannot just inject IPA as much as possible.

By the result from this chapter, four different recipes (in the case of IPA injection) for drying were used in LuCID to compare the effect of IPA on drying and stiction. To avoid any confusion, we defined specific names for each recipe. These names will be used later in this thesis:

1- Standard Recipe: 0 time injection during the delay time + 4 times injection during the drain time.
2- 1-Time Injection: 1 time injection during the delay time + 4 times injection during the drain time.
3- 2-Times Injection: 2 times injection during the delay time + 4 times injection during the drain time.
4- 3-Times Injection: 3 times injection during the delay time + 4 times injection during the drain time.
5- Double Recipe: 0 time injection during the delay time + 8 times injection during the drain time.

Standard recipe and Double recipe are able to give us an opportunity to see the effect of IPA injections during the slow drain time. In recipe 1-Time 2-Times and 3-Times Injection we are able to test the effect of IPA by increasing the number of injection during the delay time.

By the result from this chapter, **3-times Injection** recipe gave us the best result for drying the wafer since the weight of the wafer after drying with this recipe was the lowest and it shows that using more IPA can dry the wafer better.

Chapter 5 – Stiction test with Micro-Ribbons Wafer

5.1 – Aim of the chapter

In This chapter, the effect of IPA and Marangoni style drying on stiction was investigated. Micro-Ribbons Wafers with ISDP and LSN as the structural layer were released with the different etchant to find the best recipe for drying and stiction prevention.

5.2 – Micro-Ribbons Wafer with ISDP Layer

After we worked on the effect of IPA on drying, we studied on effect of IPA on stiction, which is the primary purpose of this work. The first reason to work with Micro-Ribbons Wafer was the ability of this wafer to trap water beneath the ribbons. The second usage of this test wafer is to find the effect of IPA on stiction. After wet etching, there are still droplets of water beneath these ribbons (between ribbons and surface of the silicon wafer). The width of each ribbon is 3.2 μm and the gap between each ribbon and the surface of wafer is 1.5 μm (the size of the gap corresponds approximately to the thickness of sacrificial TEOS). These droplets of water are responsible for stiction of some of the ribbons to the bottom of the cavity. Figure 5.1 shows the released ribbons. There is stiction among ribbons in this figure. As it can be seen in Figure 5.1, some ribbons are stuck to the bottom. We are looking to find a better parameters setup for LuCID to reduce the number of stuck ribbons.

(a) (b)

Figure 5.1 a) Illustration of the die with some ribbons stuck to the bottom of the cavity after etching. b) The released ribbons with no stiction. Both pictures are taken after releasing and drying. But the stiction in part (a) implies that even after drying some droplets of water may remain beneath these ribbons.

For the first step, four Micro-Ribbons Wafers with ISDP as a structural layer were used. Three of these wafers were etched with Buffered Oxide Etch (BOE) and one of them with Diluted Hydrogen Fluoride (DHF 10:1). Then during the drying process, different numbers of IPA injections were tested to find the best result and recipe for Marangoni style drying.

Considering significant number of ribbons, tens of thousands, it is difficult to determine the number of stuck ribbons by microscope. Nanometrics metrology equipment was used for this purpose. Nanometrics was defined in chapter 3.

For the first test, Micro-Ribbons Wafer with ISDP layer as a structural layer was etched with BOE. For drying, the standard recipe for LuCID Dryer was used. After that the wafer was transferred to Nanometrics. As mentioned before, in Nanometrics, the intensity of reflected light is calculated to find the height of each of ribbon. Nanometrics measured seventeen points in each wafer. Table 5.1 shows the result after drying the wafer with the standard recipe in LuCID Dryer. The results are illustrated in two parts:

1- Average height of ribbons: indicates the height of ribbons. A positive amount indicates that ribbons in average are above the wafer surface, elevated by tensile stress of the structural material, and the negative amount indicates that ribbons in average bend toward the bottom or stick to the bottom.

2- Max – Min height of ribbons: shows the difference between the highest and lowest height of ribbons in each measured position.

The situation that both average height of ribbons and the Max-Min height of ribbons are near zero is the most desirable one. This is an idealized outcome, which implies that all ribbons released perfectly and there is no bending or stiction between ribbons.

Table 5. 1 Nanometrics result for Micro-Ribbons Wafer with ISDP structural layer for standard recipe (BOE as an etchant). a) In three points (green points) among 17 measured points, the average height of ribbons is negative. It means that ribbons mostly stick to the bottom in these regions. b) In exact three points (red points) the difference height of ribbons is large. In these three red points, some of the ribbons bend upward and some of them stick to the bottom of the cavity. In these points the difference between the max and min height of the ribbons in average is 2 $\boldsymbol{\mu m}$.

Average height of ribbons

Average Height (um)								
Row	6	8	9	11	13	14	15	17
5			0.025			0.028		
7				0.027				
9	0.029		0.025		0.028			0.033
11		-0.111		0.028			0.025	
13	-0.518		0.027		0.027			-0.309
15				0.028				
17			0.027			0.026		

(a)

Max - Min height of ribbons

Somme de PV (nm)								
Row	6	8	9	11	13	14	15	17
5			39			37		
7				37				
9	31		36		33			32
11		1517		31			36	
13	2600		37		28			2466
15				29				
17			41			32		

(b)

From Table 5.1, It can be seen that from 17 measured points just three of them (highlighted in green) stuck to the bottom and the others were released. Part (b) of the table shows that exactly

in these points (highlighted in red) the difference between the maximum and minimum height of ribbons is large, but in the other points all ribbons were released with the same height. It means that in highlighted red points ribbons do not release properly and most of them stick to the bottom.

For the next test, another wafer was etched again with BOE and for drying step **3-time injection** recipe was used. The reason for trying this recipe is because of the previous experiment in chapter 4. In that experiment when 3-Times injection recipe was used, the mass of wafer after drying was the lowest among all other recipes. Table 5.2 shows the result of the **3-Times injection** recipe from Nanometrics:

Table 5. 2 Nanometrics result for Micro-Ribbons Wafer with ISDP structural layer for 3-Times injection recipe (BOE as an etchant). a) After drying with 3-Times injection recipe, in all 17 measured points there is no stiction. b) The difference of max-min height of ribbons in all 17 points is low (in average 36nm). In this recipe IPA was injected for three times during the delay time. This test shows that injection during the delay time is very efficient.

Average height of ribbons

Average Height (um)								
Row	6	8	9	11	13	14	15	17
5			0.025			0.026		
7				0.025				
9	0.027		0.026		0.021			0.028
11		0.025		0.025			0.025	
13	0.026		0.022		0.022			0.033
15				0.023				
17			0.021			0.025		

(a)

Max - Min height of ribbons

Somme de PV (nm)								
Row	6	8	9	11	13	14	15	17
5			38			34		
7				41				
9	32		32		36			38
11		40		36			39	
13	37		41		36			33
15				41				
17			42			38		

(b)

Table 5.2 shows that when we inject IPA three times during the delay time, the result is better than the result from the standard recipe. All 17 points have positive height in average and the

difference between the maximum and the minimum height of ribbons is low. Three times injection allows an IPA vapour cloud to build to a sufficient density above the water. When the recipe has three IPA injections during the delay time, the density of IPA on top of the water is more efficient to reduce the surface tension of water and make the Marangoni flow. This density of IPA (5.88×10^{19} molecule/cm^2) can flow among the ribbons better to remove the water droplets beneath these ribbons.

For the third step, we want to see the effect of IPA injection during the drain time (during the time that water goes down). In this test, there is no density of IPA on the top of the water (no injection during the delay time), and there are 8 times IPA injections during the discharge of water from the chamber (**Double Recipe**). In this situation, more IPA would spray on the surface of wafer and water during the slow drain time. Similarly to both previous tests, the wafer is designed with ISDP structural layer, but the recipe for drying after wet etching has no injection during the delay time and 8 times injections after the delay time (twice the standard recipe). Table 5.3 shows the result of this experiment.

Table 5. 3 Nanometrics result for Micro-Ribbons Wafer with ISDP structural layer for Double Recipe (BOE as an etchant). a) In seven points (green points) among 17 measured points, the average height of ribbons is negative. It means that ribbons mostly stick to the bottom in these regions. b) In 8 points (red and orange points) the difference height of ribbons is large. In four red points the difference between the max and min height of the ribbons in average is 1.1 micron. In four orange points the difference between the max and min is lower that the red points but still is high. This test shows that increasing injections during the rinse time increases stiction.

Average height of ribbons

Average Height (um)

Row	6	8	9	11	13	14	15	17
5			-0.413			-0.328		
7				0.015				
9	-0.164		0.018		0.019			0.015
11		-0.223		0.014			0.017	
13	0.018		0.027		0.018			-0.475
15				0.012				
17			-0.178			-0.334		

(a)

Max - Min height of ribbons

Somme de PV (nm)

Row	6	8	9	11	13	14	15	17
5			1021			864		
7				93				
9	1124		45		463			72
11		983		87			67	
13	78		69		66			1523
15				65				
17			903			1002		

(b)

This time, the result from Double Recipe is not as good as the previous one. As it can be seen, the average heights of ribbons in 7 points measured are negative. It means that more ribbons are stuck to the bottom and also the difference between the maximum and the minimum of the height of ribbons in 8 measured points is high. This result implies that increasing the number of injection during the slow drain time is not as effective as during the delay time. This is exactly as same as the result of the experience in chapter 4.

Similar to the experiment from the last chapter, the best result comes from the recipe with three times injections during the delay time. Here, in chapter 5, the first test wafer that was dried with the standard recipe had stiction in three points among seventeen points (as shown in Table 5.1). Afterwards, we tried to dry this released wafer again with the best drying recipe that we had found (3-Times injection recipe), to find out if we can release the three failure points or not.

For this purpose, the released test wafer was placed in the water tank for ten minutes and then it has been transferred to the LuCID with the **3-Times injection**. Table 5.4 shows the result of this experiment.

Table 5. 4 Nanometrics result for Micro-Ribbons Wafer. The first test wafer, which had been dried by standard recipe, was dried again with the best drying recipe that we found (3-time injection recipe). a) Three points that had had stiction in the first test, was released after drying with 3-time injection recipe. Unfortunately new point (green point) has stiction. b) In four points (red and orange points) the difference height of ribbons is large. In these points, some of the ribbons bend upward and some of them stick to the surface.

Average height of ribbons

Average Height (um)

Row	6	8	9	11	13	14	15	17
5			0.026			0.031		
7				0.028				
9	0.028		0.026		0.028			0.029
11		0.027		0.027			0.026	
13	0.027		0.027		0.028			0.028
15				-0.23				
17			0.025			0.025		

(a)

Max - Min height of ribbons

Somme de PV (nm)

Row	6	8	9	11	13	14	15	17
5			38			32		
7				36				
9	31		35		33			38
11		44		40			354	
13	54		41		661			46
15				1498				
17			346			43		

(b)

By comparing the result of Table 5.1 with Table 5.4, three points that had stiction in Table 5.1 released properly but one new point (the green one in Table 5.4) has a stiction. Also at four points in Table 5.4, the max-min height of ribbons has large difference. As the conclusion of this step, it shows that by drying the wafer with **3-Times injection** recipe we, potentially, could unstick these three points.

Hydrogen Fluoride (HF) is another common etchant in MEMS technology. In our cleanroom, two types of HF with a different concentration were used for etching. Diluted HF 10:1 (DHF 10:1) with lower concentration is popular etchant in wet etching. The fourth Micro-Ribbons Wafer was etched with DHF and was dried with the best recipe that we found (**3-Times injection** recipe). Table 5.5 shows the result after drying with this recipe.

Table 5. 5 Nanometrics result for Micro-Ribbons Wafer with ISDP structural layer for 3-time injection recipe (DHF as an etchant). a) Stiction occurs in all 17 points. This result shows that IPA has a different effect on stiction by changing the etchant. b) The difference between max and min height of the ribbons are a lot. It indicates that all ribbons stick to the bottom in 17 measured points.

Average height of ribbons

Average Height (um)

Row	6	8	9	11	13	14	15	17
5			-1.47			-1.47		
7				-1.46				
9	-1.47		-1.46		-1.46			-1.46
11		-1.46		-1.47			-1.45	
13	-1.46		-1.46		-1.46			-1.47
15				-1.45				
17			-1.45			-1.45		

(a)

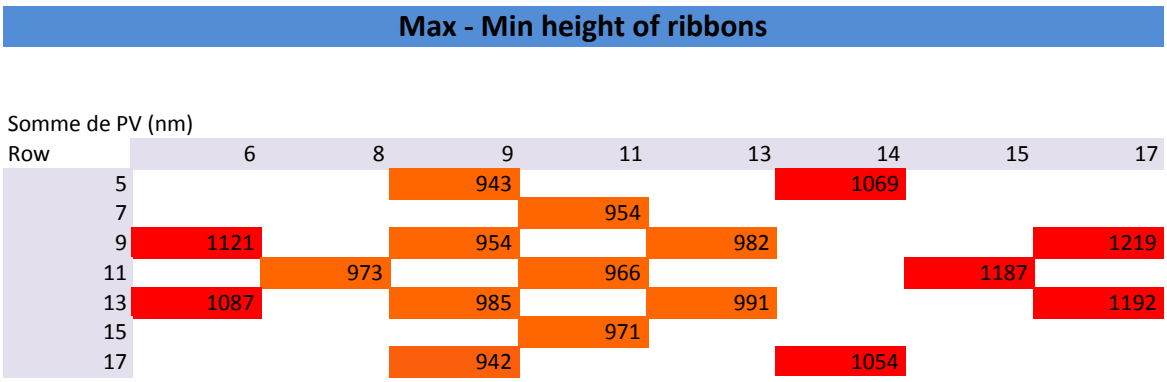

(b)

The result of drying the test wafer after etching in DHF 10:1 are significantly worse compared to previous 3 tests, since all 17 measured points illustrated stiction. The result is totally different than the result from BOE. This test shows that IPA has a different effect on stiction by changing the etchant**. 3-Times injection** recipe gives us a good outcome after etching by BOE due to the stiction. We expect that this recipe will be good for DHF. But the result was not consistent with this statement. We also fabricated Micro-Ribbons test wafers with LSN structural layer. In the following section, we will discuss about these test wafers and their result.

5.3 – Micro-Ribbons Wafer with LSN Layer

As mentioned before, two types of structural layer have been used to fabricate the Micro-Ribbons wafer. In previous tests, discussed earlier, all test wafers had ISDP layer as a structural layer, and the sacrificial layer was etched by BOE and DHF. For the next step, we tried to release wafers with LSN as a structural layer using the same etchants, BOE and DHF. Unfortunately, as is shown in Table 5.6, in all seventeen points we had stiction. **Standard Recipe**, **Double Recipe**, and Recipe **3-Times injection** have been tried and in all recipes the all measured points had stiction. The table below shows the result of the standard recipe. In all wafer with LSN as the structural layer, the results were same.

Table 5. 6 Nanometrics result for Micro-Ribbons wafer with LSN as the structural layer for the standard recipe. This is the result of just one wafer but in all other wafers with LSN as a structural layer, stiction had happened in all 17 points.

LSN layer is a transparent layer and because Nanometrics device uses light to measure the height of surfaces, taking the measurement with these wafers is very difficult. The main reason for the failure of releasing ribbons with LSN layer could be attributed to the thickness of LSN layer. As described before, the thickness of LSN is 435nm, which is so thin and sensitive, that after etching the oxide layer (sacrificial layer), the cavity beneath the ribbons is around 1.5 microns and the stiction is inevitable. Figure 5.2 shows the picture of released ribbons with LSN layer on top:

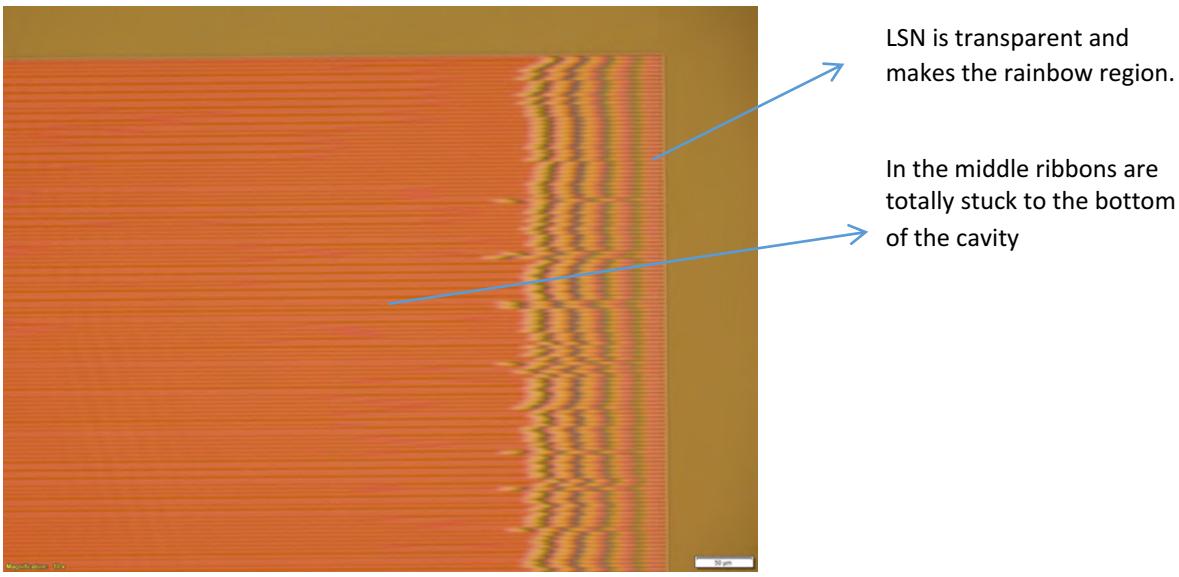

Figure 5. 2 Released Micro-Ribbons with LSN layer as a structural layer. The main reason for the failure of releasing ribbons with LSN layer is because of the thickness of LSN layer. LSN layer is so thin (435 nm).

One wafer also was etched with DHF and was dried with Recipe **3-time injection**, and again the result was as same as the previous one. Stiction was registered in all measured points.

5.4 – Result and discussion

As the conclusion of the Micro-Ribbons wafers experiment, two types of the structural layer with different recipes were dried. Wafers were etched with BOE and DHF as an etchant. For test wafers with LSN layer as a structural layer, four different types of drying recipes were tried. But stiction had occurred in all test wafers.

For the wafers with ISDP layer, the best recipe was **3-times injection** recipe. With this recipe, there was no stiction in all 17 points. Increasing the number of injection during the drain time increases the number of stuck points but increasing the number of injection during the delay time decreases the number of stuck points.

This test also shows that different etchant needs a different type of recipe for drying. The **3-time injection** recipe was found the best recipe for BOE as an etchant but the outcome for DHF was entirely different.

This result encouraged us to find the best recipe for DHF and compare it with the best recipe for BOE. For the next step, we decided to test the stiction on test wafers with cantilevers in different lengths and widths.

Chapter 6 – Stiction test with Cantilevers Wafer

6.1 – Aim of the chapter

In this chapter, the further studies on the effect of IPA and Marangoni style drying on stiction are presented. Engineered Cantilever Wafers (Cantilever-Wafer) with ISDP as the structural layer were released with different etchant to find the best recipe for drying due to the stiction. For the final Step, contaminant measurement was investigated to see if using LuCID increases the contamination.

6.2 – Cantilevers wafer with ISDP layer

6.2.2 – Stiction test with Cantilevers Wafer

In the last chapter (Micro-Ribbons Wafer) ribbon in all 17 points stick to the bottom of the cavity after releasing with DHF, and this result encouraged us to work more on this etchant. This time, we concentrate more on releasing wafer with DHF to find the best recipe for this etchant. For the beginning, wafers were released with DHF and by inspection with visible range device (Rudolph), which was described in chapter 3, the number of defects was measured after each drying recipe. When the released cantilevers moved from their original place even in nanometre dimension, Rudolph finds the cantilevers as a defect and counts a number of defects in this way.

For the first test, the structures were released with DHF and dried with the **standard recipe**. For the **standard recipe**, the number of defects was 1954. Because in the previous experiment, **3-time injection** recipe gave us the best result for BOE as an etchant, the second wafer was dried with this recipe. Again, exactly like the previous test in chapter 5, the number of defects was

increased after using **3-time injection** recipe for DHF as an etchant. This time, the number of defects was 2593.

In this experiment, the best result has come from the recipe with just one-time injection during the delay time and then four times injection during the rinse time (Recipe **1-time injection**). The number of defects was 1148. When the number of injection during the delay time is two times (**2-time injection**), the number of defects increases to 2326. Figure 6.1 shows the number of defects with a different type of injection for drying.

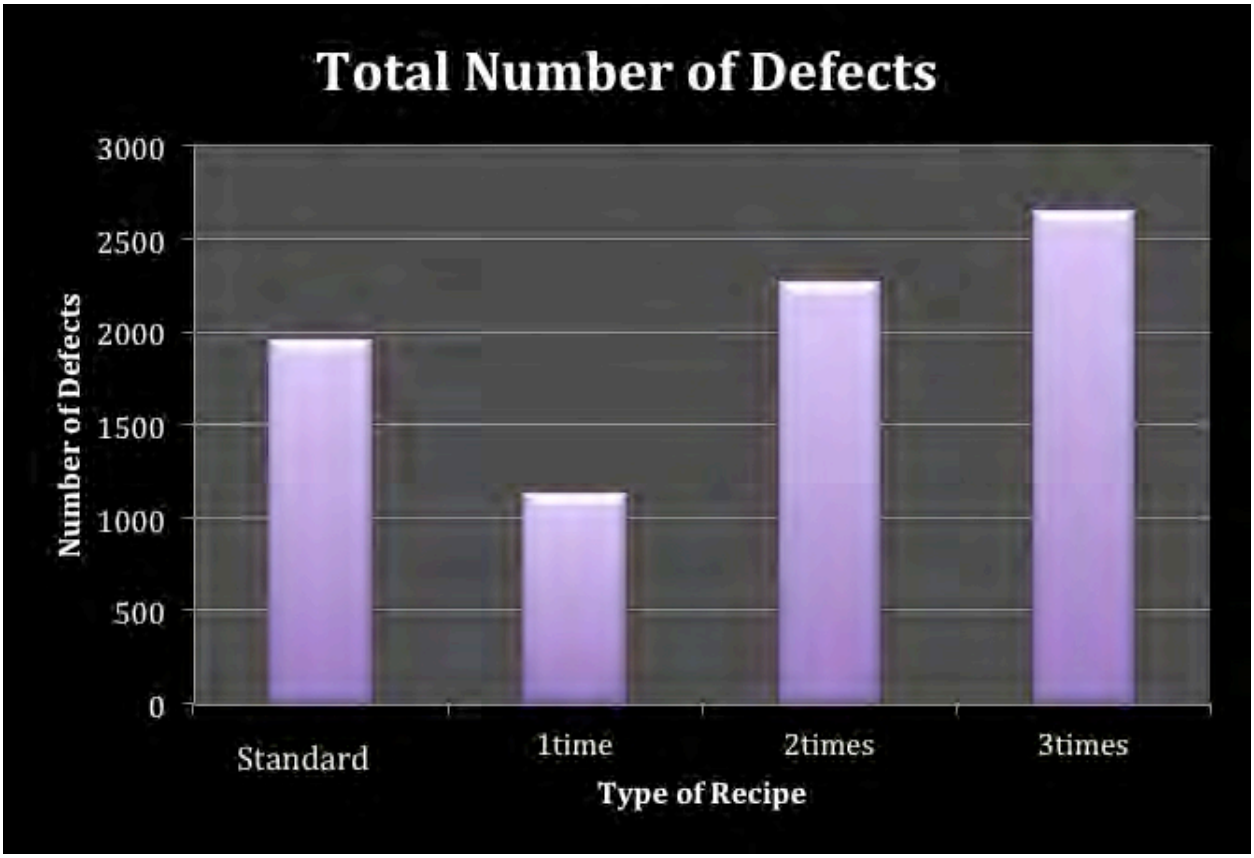

Figure 6. 1 Total number of defects after releasing cantilevers with different type of recipe (Etchant DHF). 1-time injection recipe gives the lowest number of defects.

As mentioned before, for releasing the cantilevers the etchant that has been used was DHF. For the next step in this experiment, one wafer was released with BOE, and was dried with the best recipe that had been found in the previous section (**3-time injection** recipe). This time, the number of defects decreased enormously. Figure 6.2, shows the result after etching the wafer

with BOE with **3-time injection** recipe and compared its result with the best result of **1-time injection** recipe and standard recipe with DHF as an etchant.

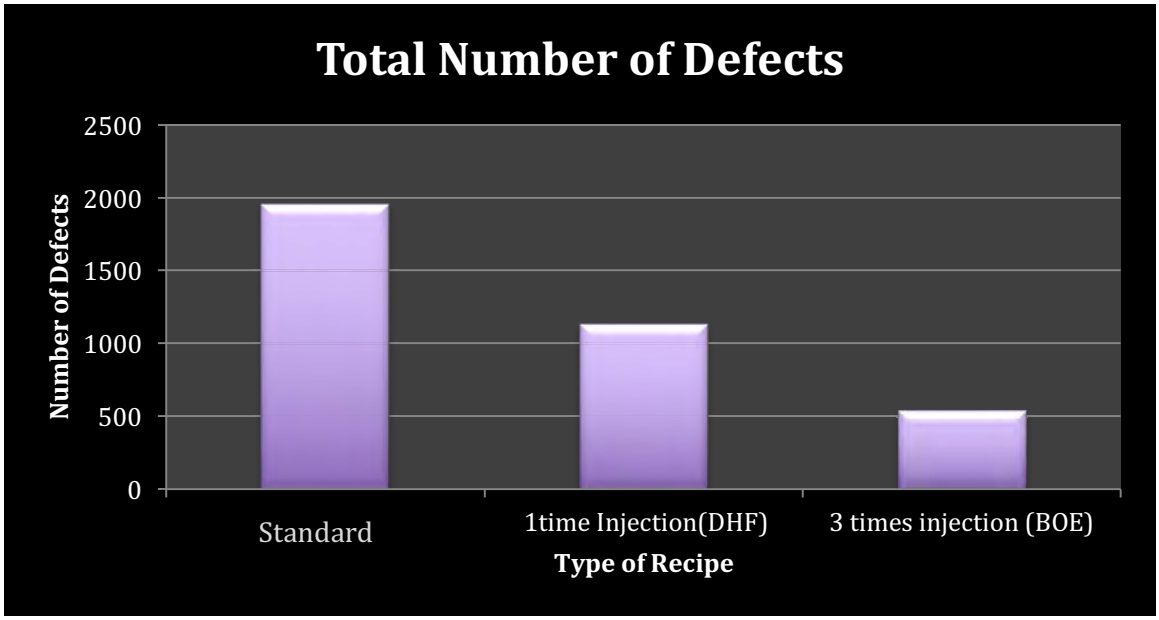

Figure 6. 2 Comparison of number of defect with different etchant and different type of recipe. This result shows that different type of etchant needs a different kind of recipe for drying.

Figure 6.2 shows that different type of etchant needs a different kind of recipe for drying. This experiment implies that for BOE we need more concentration of IPA at the surface of the water than DHF.

In all drying recipes, we concentrate more on the number of injection during the delay time. The first experiment it showed that, increasing the number of injection during the slow drain time does not have a significant effect on drying in comparison with the injection during the delay time.

As described in chapter 2, during the rinse time water goes down with the speed of 1 mm/s and during this period, there are numbers of injection depending on a recipe. The diameter of our silicon wafer was 200 mm, and it contains rows of dies with structures location schematically illustrated in Figure 6.3:

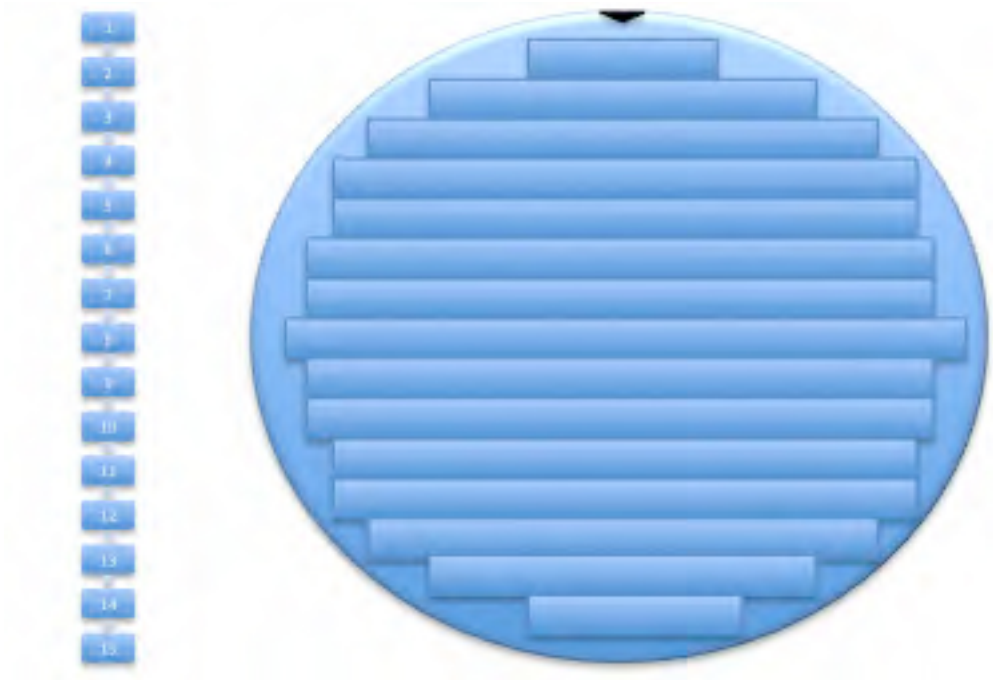

Figure 6. 3 Rows of dies in Cantilevers Wafer. There are 15 rows of die in each wafer. In each row, there are numbers of dies.

The Engineering test wafer contains 15 rows of dies and in each die, as described before, there are three columns of smaller dies that contain cantilevers with different width shown in Figure 6.4.

The width of the cantilevers on top smaller die is 1.5 micron; the middle one is 2.5 micron, and the bottom one is 3.5 micron. In each die, there are cantilevers with various lengths from 30 to 600 microns.

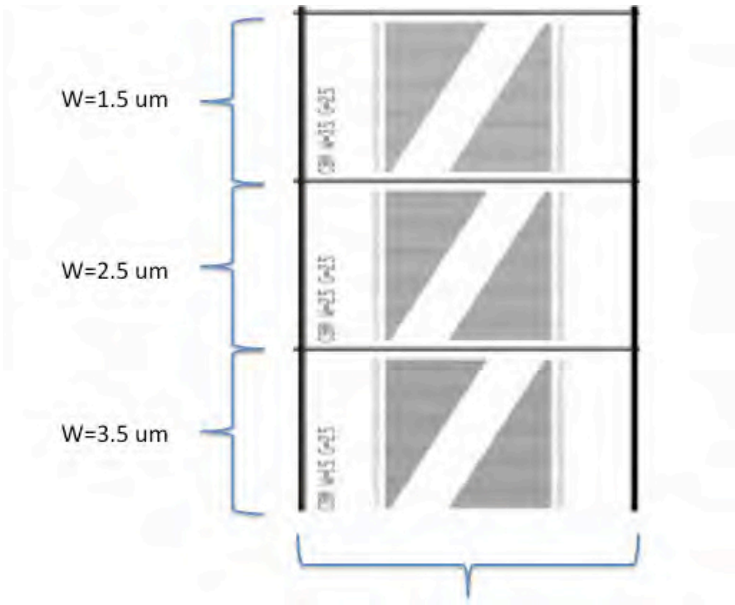

Figure 6. 4 Cantilevers with different widths. Inside each die there are three smaller dies. Each of these smaller die has cantilevers with various widths (1.5, 2.5 and 3.5 microns).

This structure gives us an opportunity to inspect the wafer from the top to the bottom (exactly at the middle die) by microscope and see the effect of injection during the rinse time on stiction.

For this purpose, we count the number of cantilevers not affected by stiction inside each smaller die using the microscope. Figure 6.5 shows the number of unaffected cantilevers from the top to the bottom of the wafer.

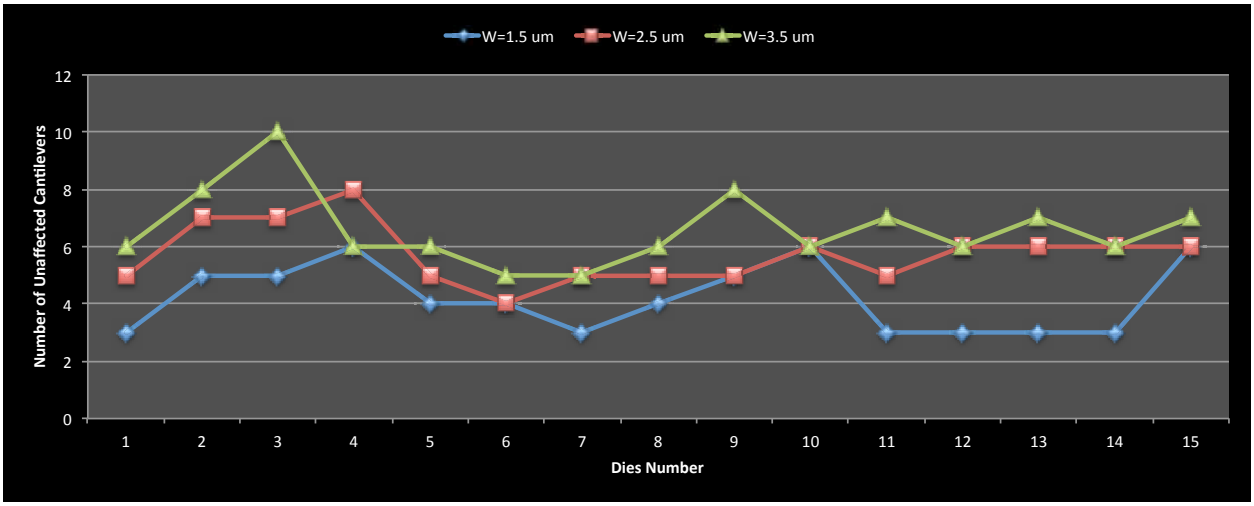

Figure 6. 5 Number of unaffected cantilevers (drying with standard recipe) shown for 3 different cantilever widths of $\boldsymbol{W = 1.5\ \mu m}$ (Blue), $\boldsymbol{W = 2.5\ \mu m}$ (red) and $\boldsymbol{W = 3.5\ \mu m}$ (Green). By microscope, the number of unaffected cantilevers was counted inside each smaller die from top to the bottom of a wafer. The highest number of unaffected cantilever for the standard recipe is ten.

In Figure 6.5, the number of the unaffected cantilevers for each die and each width corresponds to the cantilevers that do not stick to either bottom of the cavity or to the side among the total 58 cantilevers.

Figure 6.5 shows that the highest number of the unaffected cantilevers with the **standard** recipe is ten cantilevers. It means that using the **standard** recipe the highest lengths of the unaffected cantilever is 120 microns. Since the smallest cantilever in our test wafer is 30 microns so the length of tenth cantilever is 120 microns.

Taking to consideration that there are four injections during the slow drain time, we can divide the wafer from top to the bottom into four parts. So the first injection covers die from number 1 to number 4, the second injection covers from 4 to 8, and it continues till die 16.

By this definition Figure 6.5 implies that in the first injection during the slow drain time, the effect of IPA on drying is much higher than the effect of IPA during the later injections. This situation implies that the speed of slow drain is still too fast. It means that for the first injection, vaporized IPA can reach the surface properly from the tank's lid to the surface of the water. However, the subsequent injections are not able to reach the surface perfectly and because of that starting at row of dies number 4 (Fig. 6.5), the numbers of unaffected cantilevers do not change specifically.

6.3 – Contaminant measurement

For the last step, it is important to see how effective the LuCID Dryer in removal of all contaminants. For this purpose, XPS device was used to measure the number of contaminants. To do the contaminants measurement, three new silicon wafers, which we call them wafer 20, 22 and 24 were used.

The first wafer (Wafer 20) was placed in LuCID Dryer and IPA was injected on its surface with the standard recipe. On the second wafer (Wafer 22) the layer of oxide was deposited on the surface of the wafer. This process is called Plasma Etching. In plasma etching the plasma oxidized the wafer surface, adding oxygen and masking the silicon substrate. Finally, for the last wafer (wafer 24), it was treated with the oxygen plasma (plasma etching) and then this wafer was

placed in LuCID Dryer. Again, in LuCID dryer, **standard** recipe has been used to inject IPA four times during the drain time.

From each wafer, three samples with the size of 70 × 70 mm were taken and placed in XPS device. So the arrangement of samples is shown below.

-XPS analysis of 3 samples (from center area of 3 wafers):

- Wafer 20 (IPA): three samples A, B and C
- Wafer 22 (plasma + IPA): three samples A, B and C
- Wafer 22 (plasma): three samples A, B and C

Normally, to check contaminants on wafer's surface carbon, oxygen and silicon is very important. On each sample, a survey (200µm spot) was done on 3 different sites and high-energy resolution spectra (C, O, Si) was done on another site. The Figures 6.6 and 6.7 show the results of XPS measurement.

		Relative Atomic Concentration (%at)			
Description		[C]	[O]	[Si]	[F]
W20 - IPA	A	16.7	32.7	50.3	0.3
	B	15.7	32.5	51.5	0.3
	C	13.2	33.3	53.1	0.3
W22 - plasma & IPA	A	9.1	51.9	38.6	0.4
	B	8.8	51.3	38.8	1.0
	C	9.5	51.0	38.9	0.6
W24 - plasma	A	10.6	50.2	39.3	
	B	8.3	51.8	39.9	
	C	9.9	50.6	39.5	

Figure 6. 6 The result of XPS measurement on three wafers.

Both samples with oxygen plasma on their surface, wafer 22 and 24, have similar surface composition and practically identical chemical states for carbon, silicon and oxygen. Injection IPA after plasma does not add more carbon or change the carbon species at the surface after plasma.

The unexpected situation happens when both samples with IPA injection, wafer 20 and 22, show trace of fluorine. It is not detected on sample with plasma only.

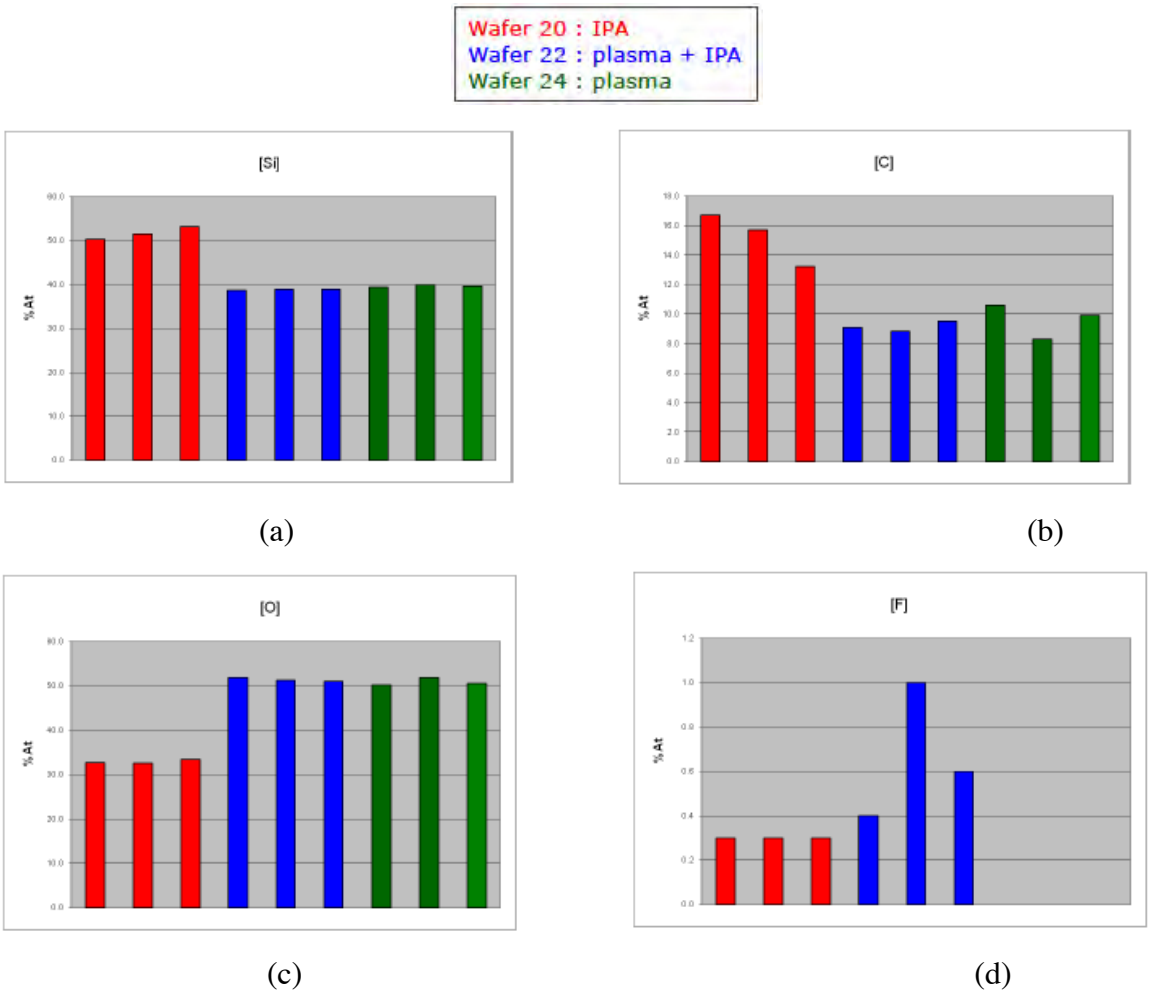

Figure 6. 7 Atomic concentration of silicon on the surface of each sample. a) silicon, b) carbon, c) oxygen, d) fluorine. The charts show that LuCID does not add contaminants such as silicon, carbon and oxygen on the surface of each sample. However, fluorine has been found on the samples that IPA was injected on them.

This experiment shows that, LuCID Dryer does not add any contaminant, only the trace of fluorine has been seen at surface of wafer that IPA were sprayed on their surfaces. The problem may be because of the LuCID's tank. The tank of LuCID is made of poly-vinylidene difluoride (PVDF) with the chemical formula $(C_2H_2F_2)_n$. It is possible IPA has an effect on this chemical structure and release fluorine on the surface of the wafer. This problem may be also due to the fact that the DI water rinse cycle may not be sufficient and further tests might be necessary.

6.4 – Result and Discussion

In this study, Cantilevers Wafer with ISDP structural layer was used as a test wafer. In this chapter we concentrate more on releasing wafer with DHF to find the best recipe for this etchant. As the conclusion of Cantilevers Wafer experiment, in this test, the best result has come from the recipe with just one-time injection during the delay time (**1-time injection** recipe).

This test shows that different type of etchant needs a different kind of recipe for drying. This experiment implies that for BOE we need more concentration of IPA at the surface of the water than DHF.

In addition, we speculate that the speed of a slow drain could be optimized to accommodate the effect of IPA injections. During the first injection, sprayed IPA can reach the surface of water properly, and because of that the number of cantilevers unaffected by stiction is around ten. However, after the first IPA injection and, supposedly, because the speed of draining water is elevated, during the second and following injections IPA cannot reach the surface of water properly. This could be a reason why the number of unaffected cantilevers is reduced to seven.

Furthermore, we found that LuCID is able to remove the contaminants perfectly but only the trace of fluorine has been seen on the surface of wafers that IPA was sprayed on them.

Chapter 7 – Stiction Experiment

7.1 – Aim of the chapter

The deflection, mechanical stability and adhesion of cantilevers are investigated in this chapter. The magnitude and the effect of both capillary force and intersolid adhesion in companion with experimental data for Polysilicon cantilevers are presented in this chapter.

7.2 - Experimental result and discussion:

As it was described before the cantilever wafer contains cantilevers with different widths, lengths and gaps. This special test wafers give us an opportunity to test the equation 7 and 8 introduced in chapter 1. The surface layer of these test wafers was Polysilicon. During the fabrication process, the oxide layer was sacrificially etched in a DHF (10:1) bath to release the beams, and the samples were rinsed thoroughly. The wafers from the rinse were hydrophobic due to the HF etch. After releasing the cantilevers, the detachment length (L_d) of the microstructures was detected under a microscope. By the method was described in section 1.9, L_d was plotted for each drying situation.

For all calculation these values are necessary:

- For hydrophobic Polysilicon layer: γ_s= 100 $\pm$ 60 mJm^{-2} [21].
- The Young's Modulus for LPCVD ISDP structural layer, n + type (phosphorous doped): E = 170 $\pm$ 10 GPa [40].
- The liquid surface tension of water 72.01 mJm^{-2} at 25°C [24].
- The liquid surface tension of IPA 21.2 mJm^{-2} at 25°C [24].

The first cantilever wafer was dried with pure water (no IPA). Fig. 7.1 shows a plot of the detachment length, L_d, versus the parameter $\left[\frac{h^2t^3}{(1+\frac{t}{w})}\right]^{1/4}$ for hydrophobic samples. The Slope of the line corresponds to the value of $\left[\frac{2E}{9\gamma_L \cos\theta_c}\right]^{1/4}$ predicted by the equation.

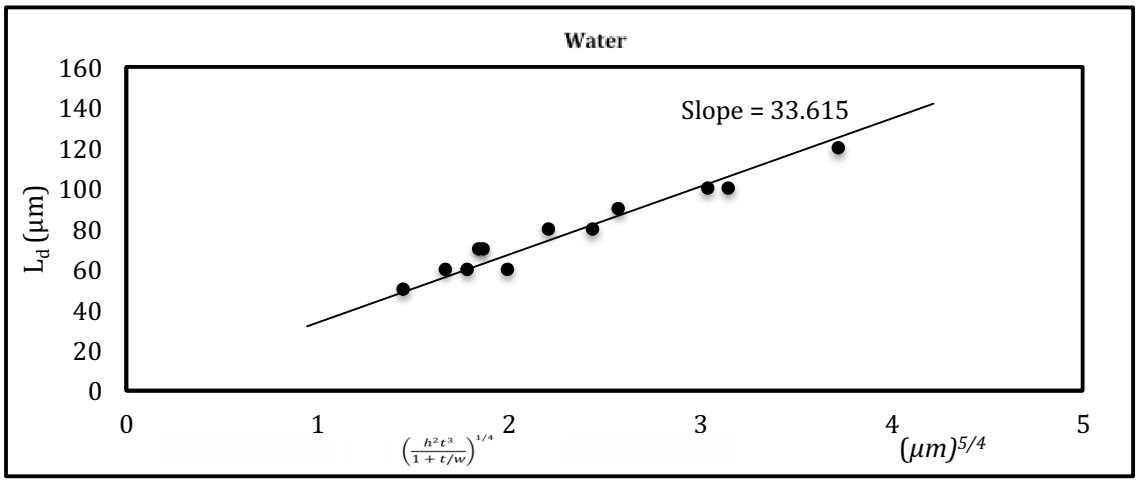

Figure 7. 1 Plot of the detachment length, $\boldsymbol{L_d}$, versus $\left[\frac{\boldsymbol{h^2t^3}}{(1+\frac{t}{w})}\right]^{\boldsymbol{1/4}}$ for pure water.

Because we have the value of E (Young's Modulus), we are able to calculate the value of $\gamma_L \cos\theta_c$.

$\gamma_L \cos\theta_c$ = 29.587 mJm^{-2} and for pure water $\gamma_L = 72.01$ mJm^{-2} $\rightarrow$ $\theta_c = 114.3\ °C$.

Fig. 7.2 shows plot of the experimental detachment length, L_d, as a function of the parameter $(h^2t^3)^{\frac{1}{4}}$ for hydrophobic cantilever-beam samples. From (4), the slope of this curve is obtained setting N_p = 1 and equal to $\left(\frac{3E}{8\gamma_s}\right)^{1/4}$. The observed value of L_d was independent of the beam width, w. As mentioned before the value of γ_s for hydrophobic surface is 100 ± 60 mJm^{-2} and has to be constant for any liquid.

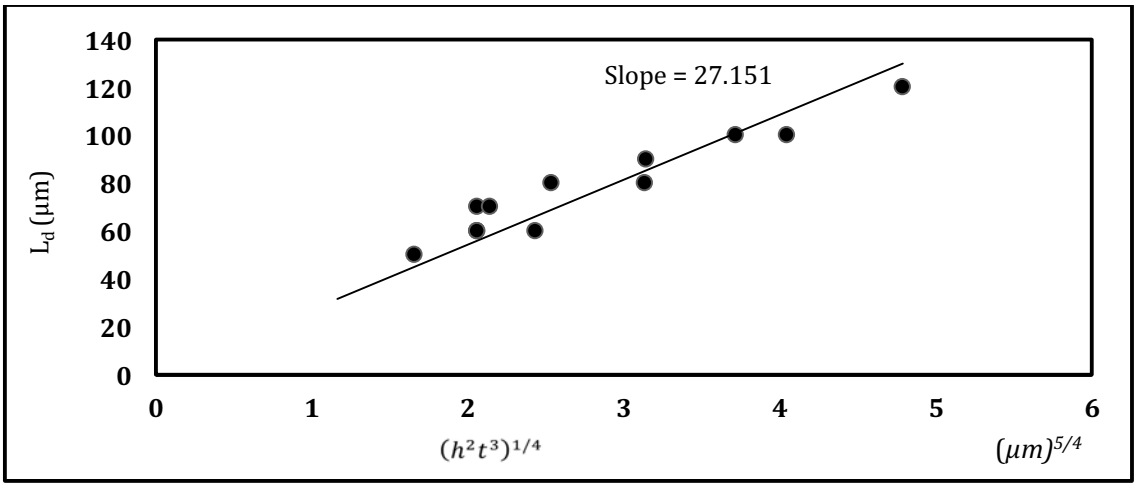

Figure 7. 2 Plot of the experimental detachment length, L_d, as a function of the parameter $(h^2t^3)^{\frac{1}{4}}$ in pure water.

The slope of our experimental result is 27.151. Therefore, the value of $\gamma_s = 117.3$ mJm^{-2} which agrees with previous works.

The second sample wafer was dried with 3-Times injection Recipe. The concentration of IPA after 3 times injection is $5.88\times10^{19}\ molecule/cm^2$. Fig 7.3 shows a plot of the detachment length, L_d, versus the parameter $\left[\frac{h^2t^3}{(1+\frac{t}{w})}\right]^{1/4}$ for samples dried with 3-Times injection. After calculation, the value of $\gamma_L \cos\theta_c$ is 21.8.

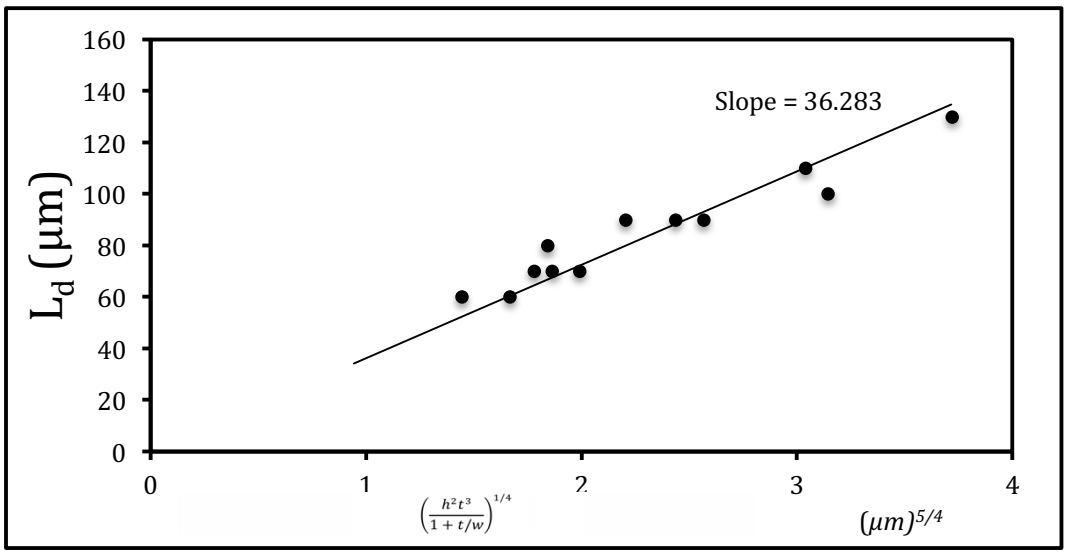

Figure 7. 3 Plot of the detachment length, L_d, versus $\left[\frac{h^2t^3}{(1+\frac{t}{w})}\right]^{1/4}$ for 3-Times IPA injection.

Fig. 7.4 shows plot of the experimental detachment length, L_d, as a function of the parameter $(h^2t^3)^{\frac{1}{4}}$ for samples is dried with 3-Times injection. According to the theoretical equation, γ_s must be constant.

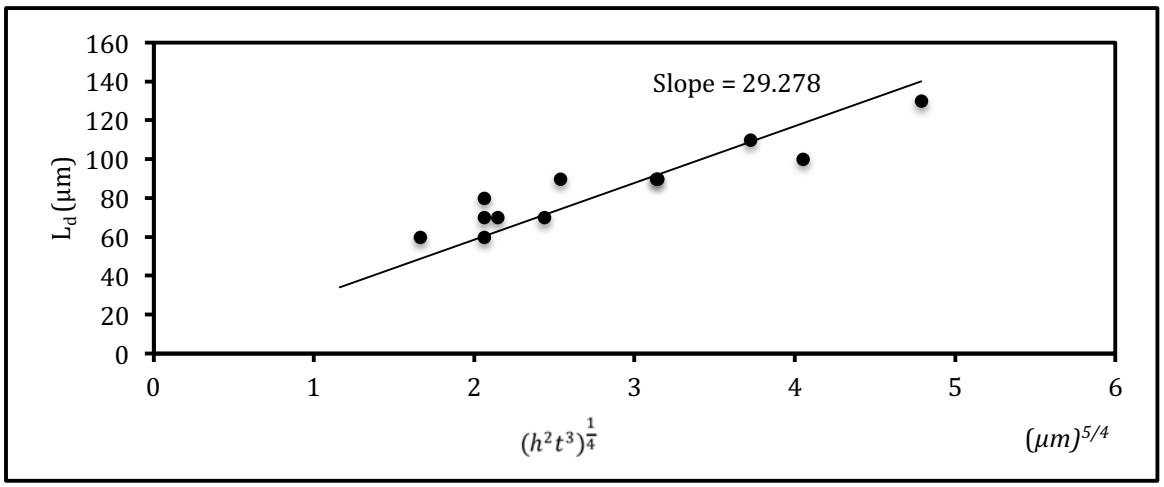

Figure 7. 4 Plot of the experimental detachment length, $\boldsymbol{L_d}$, as a function of the parameter $\boldsymbol{(h^2t^3)^{\frac{1}{4}}}$ for 3-Times Injection.

We expect that the value of $\gamma_s$does not change according to the theoretical equation. But the experimental result indicates that the value of γ_s decreases to 86.8 mJm^{-2}

This result is similar to the work has been done by O. Raccurt *et al*. In their work the value of γ_s also has been changed for various liquids for drying (water, IPA, pentane).

For the third step, we dried the samples with 2-Times Injection Recipe. The concentration of IPA on top of the water is $3.92\times10^{19}\ molecule/cm^2$. Fig. 7.5 and Fig. 7.6 show a plot of the detachment length, L_d, versus the parameter $\left[\frac{h^2t^3}{(1+\frac{t}{w})}\right]^{1/4}$ and $(h^2t^3)^{\frac{1}{4}}$ for samples dried with 2times injection.

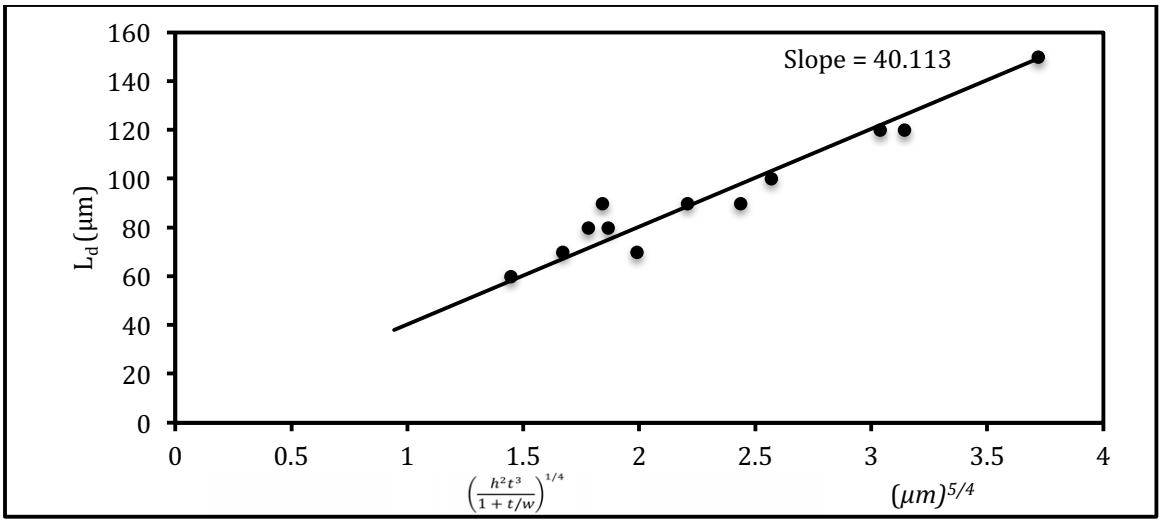

Figure 7. 5 Plot of the detachment length, $\boldsymbol{L}$, versus $\left[\frac{\boldsymbol{h^2t^3}}{(\boldsymbol{1+\frac{t}{w}})}\right]^{\boldsymbol{1/4}}$ for 2-Times IPA injection.

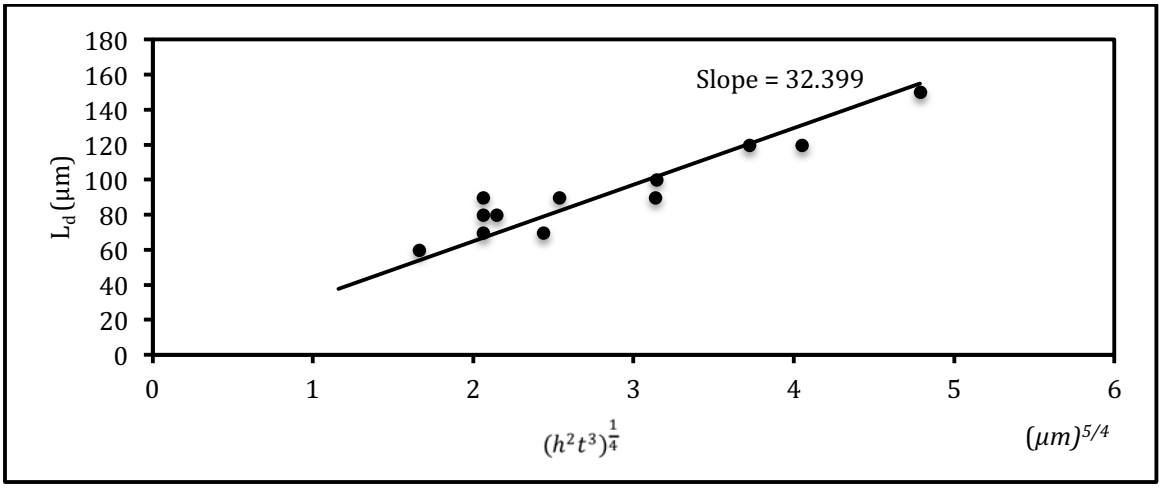

Figure 7. 6 Plot of the experimental detachment length, $\boldsymbol{L_d}$, as a function of the parameter $(\boldsymbol{h^2t^3})^{\frac{1}{4}}$ for 2-Times IPA injection.

After calculation, the value of $\gamma_L \cos\theta_c$ is 14.6 and γ_s is 59.4.

Finally for the last step, we dried the samples with 1-Time Recipe. The concentration of IPA on top of the water is $1.96\times10^{19}\ molecule/cm^2$. Fig. 7.7 and Fig. 7.8 show a plot of the detachment length, L_d, versus the parameter $\left[\frac{h^2t^3}{(1+\frac{t}{w})}\right]^{1/4}$ and $(h^2t^3)^{\frac{1}{4}}$ for samples dried with 1time injection.

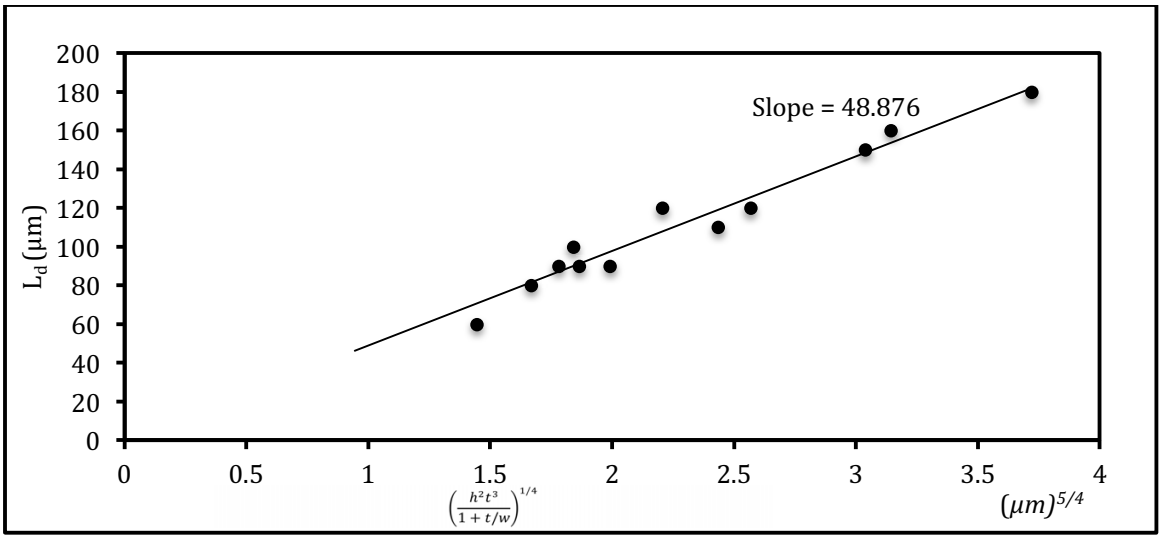

Figure 7. 7 Plot of the detachment length, $\boldsymbol{L_d}$, versus $\left[\frac{h^2t^3}{(1+\frac{t}{w})}\right]^{1/4}$ for 1-Time IPA injection.

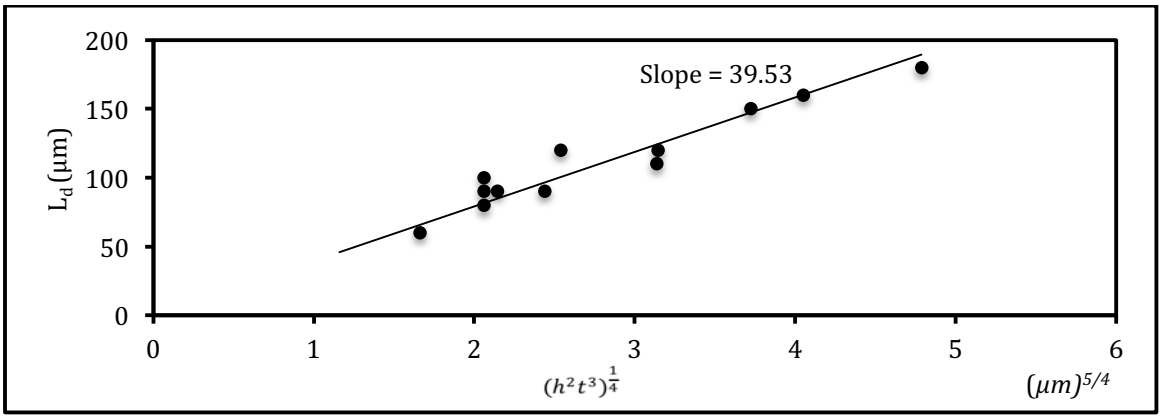

Figure 7. 8 Plot of the experimental detachment length, $\boldsymbol{L_d}$, as a function of the parameter $(\boldsymbol{h^2t^3})^{\frac{1}{4}}$ for 1-Time IPA injection.

After calculation, the value of $\gamma_L \cos\theta_c$ is 6.62 and γ_s is 26.1. All graphs were plotted together for both N_{EC} and N_P to see the difference better.

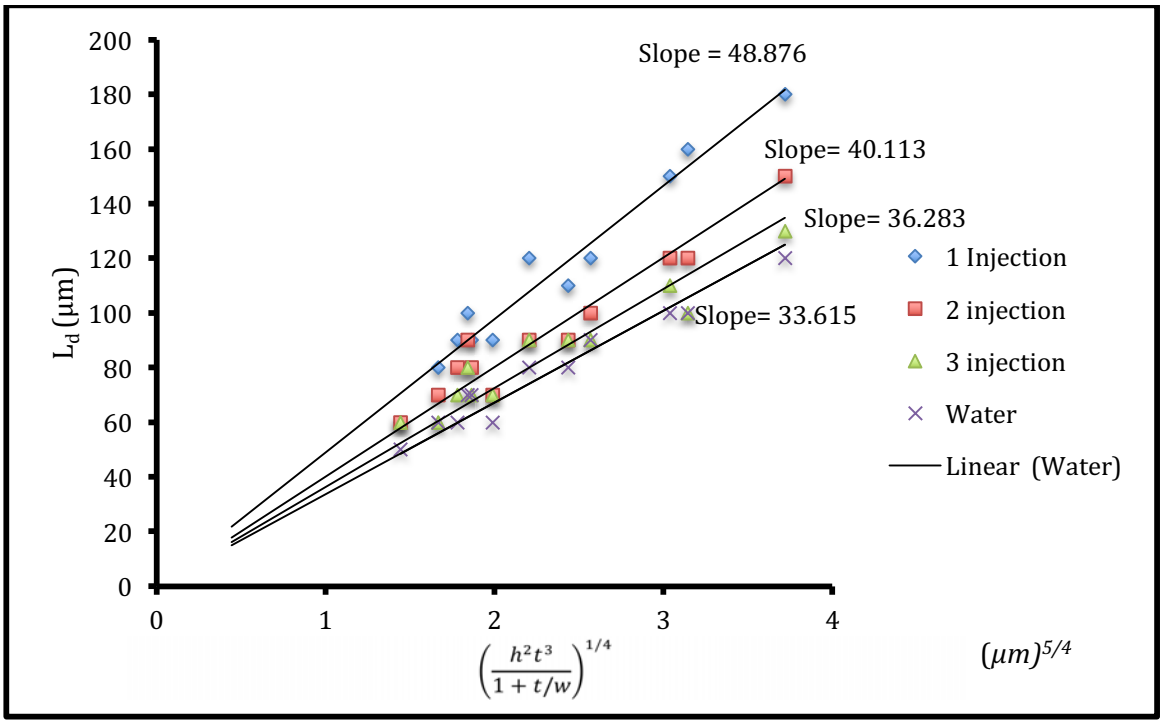

Figure 7. 9 Plot of the detachment length, L_d, versus $\left[\frac{h^2t^3}{(1+\frac{t}{w})}\right]^{1/4}$ for all types of drying.

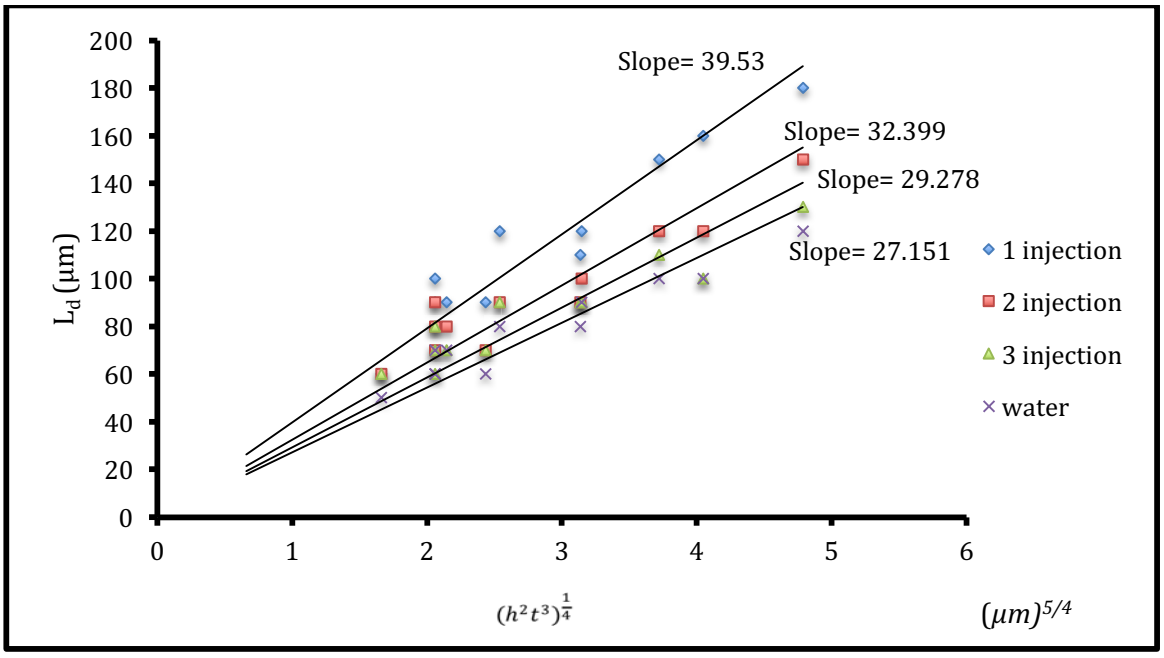

Figure 7. 10 Plot of the experimental detachment length, L_d, as a function of the parameter $(h^2t^3)^{\frac{1}{4}}$ for all types of drying.

The table below shows all the results from different recipes together:

Table 7. 1 Summary of information extracted from experimental results

Water	Slope (N_{EC})= 33.615 Slope (N_P) = 27.151	$\lvert \gamma_L \cos\theta_c \rvert = 29.587$ $\gamma_{L(water)} = 72.1\ \mathrm{mJ}m^{-2}$ $\theta_c = 114.3\ °C$	Calculated surface tension $\gamma_s = 117.3$	
3 IPA injection	Slope (N_{EC}) = 36.283 Slope (N_P) = 29.278	$\lvert \gamma_L \cos\theta_c \rvert = 21.8$ $50 < \gamma_{L(mixture)} < 72\ \mathrm{mJ}m^{-2}$ $108° < \theta_c < 116° \rightarrow \theta_c \sim 112°$	Calculated surface tension $\gamma_s' = 86.8$	$\gamma_s' \sim \lvert \cos\theta_c \rvert$
2 IPA injection	Slope (N_{EC}) = 40.113 Slope (N_P) = 32.399	$\lvert \gamma_L \cos\theta_c \rvert = 14.6$ $50 < \gamma_{L(mixture)} < 72\ \mathrm{mJ}m^{-2}$ $102° < \theta_c < 107° \rightarrow \theta_c \sim 105°$	Calculated surface tension $\gamma_s' = 59.4$	$\gamma_s' \sim \lvert \cos\theta_c \rvert$
1 IPA injection	Slope (N_{EC}) = 48.876 Slope (N_P) = 39.53	$\lvert \gamma_L \cos\theta_c \rvert = 6.62$ $50 < \gamma_{L(mixture)} < 72\ \mathrm{mJ}m^{-2}$ $95° < \theta_c < 98° \rightarrow \theta_c \sim 96.5°$	Calculated surface tension $\gamma_s' = 26.1$	$\gamma_s' \sim \lvert \cos\theta_c \rvert$

Table 7.1 shows that when IPA is mixed with water during the drying process, liquid surface tension is reduced. In LuCID the concentration of IPA in all different type of recipe is less than 5%. Table 1.1 implies that when the concentration of IPA is less than 5%, the surface tension of the mixture is between 50 and 72 mJm^{-2} at $25°C$. So for all recipes that contains IPA injection, we assumed that $50 < \gamma_{L(mixture)} < 72\ \mathrm{mJm}^{-2}$.

As a result, it can be seen that:

1- After having IPA injection, the value of $\lvert \gamma_L \cos\theta_c \rvert$ is less than the value of $\lvert \gamma_L \cos\theta_c \rvert$ with pure water as predicted.

2- By reducing the number of IPA injections, the value of $\lvert \gamma_L \cos\theta_c \rvert$ is decreased. This situation shows the influence of contact angle. Although by having more IPA injection, liquid surface tension getting lower, the contact angles increases. Because of that the total value of $\lvert \gamma_L \cos\theta_c \rvert$ is getting lower by decreasing the number of IPA injection (even less than the liquid surface tension of IPA). This result shows that the contact angle has an important role in stiction.

3- The interesting phenomenon happens for solid surface tension γ_s during IPA injection. This value is not constant and by having IPA injection, the surface tension is getting

lower than the value of γ_s for water and we call it γ_s'. However, there is a relation between γ_s' and $\cos\theta_c$. In all three types of recipes $\gamma_s' \sim |\cos\theta_c|$.

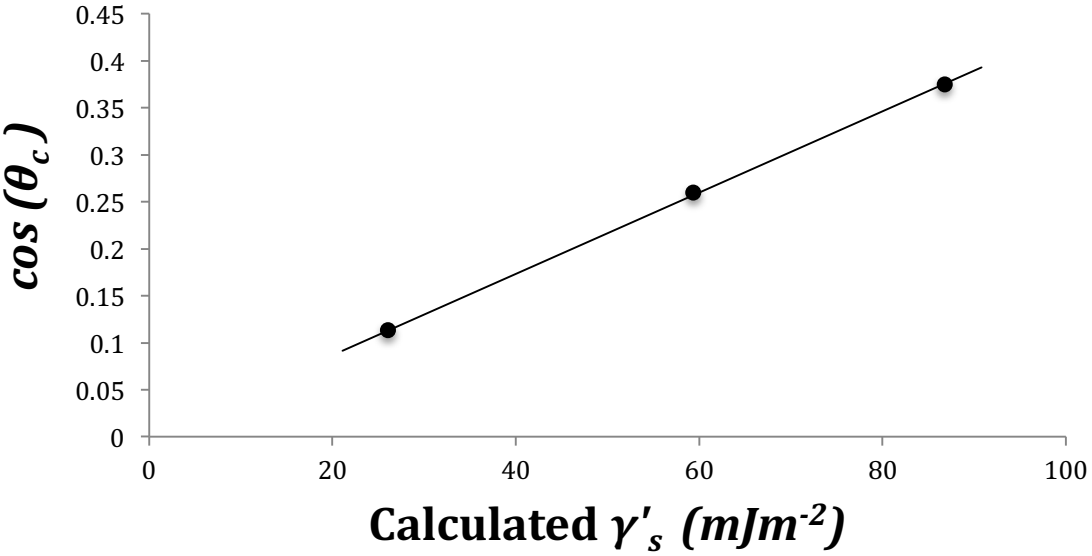

Figure 7. 11 Calculated Solid surface tension versus the value of $|\cos\theta_c|$

The other important phenomenon is work of adhesion. As described earlier work of adhesion represents the work necessary to separate a drop from the solid surface. Work of adhesion depends on liquid surface tension and contact angle as is shown in equation below:

$$W_{AB} = \gamma_l\,(1 + \cos\theta_c)$$

We assumed that liquid surface tension is the same for all three types of recipe (actually, γ_l reduces by increasing the number of injection but the total value of surface tension would be between 50 and 72 mJm^{-2}). The calculated contact angle was illustrated in Table 7.1. In Table 7.2, the value of work of adhesion is calculated for each recipe.

Table 7. 2 For each recipe the value of γ_L was assumed between 50 and 72 mJm^{-2}. Contact angle was calculated in previous table. For each type of recipe, work of adhesion is calculated in the last column.

Number of Injection	Liquid Surface Tension ($\mathrm{mJ}m^{-2}$)	Contact Angle	Work of Adhesion ($\mathrm{mJ}m^{-2}$)
3 IPA injection	$50 < \gamma_{L(mixture)} < 72$ $\gamma_L = 61$	$108° < \theta_c < 116° \rightarrow \theta_c \sim 112°$	$W_{AB} = 38.15$
2 IPA injection	$50 < \gamma_{L(mixture)} < 72$ $\gamma_L = 61$	$102° < \theta_c < 107° \rightarrow \theta_c \sim 105°$	$W_{AB} = 44.47$
1 IPA injection	$50 < \gamma_{L(mixture)} < 72$ $\gamma_L = 61$	$95° < \theta_c < 98° \rightarrow \theta_c \sim 96.5°$	$W_{AB} = 54.1$

Table 7.2 shows that by increasing the number of IPA injection, W_{AB} is decreasing. It means that when we have more concentration of IPA on the surface of water, separating water from a solid surface is easier.

In the last experiment we used two test wafers with the structures illustrated in the figure below to test the stiction for both hydrophilic and hydrophobic surfaces.

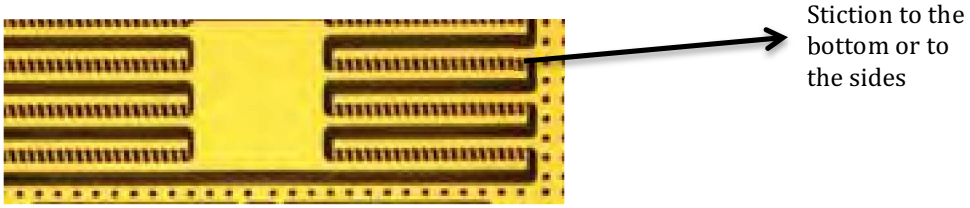

Figure 7. 12 Test wafer to test the stiction for both hydrophilic and hydrophobic surfaces.

The first test wafer was placed in Standard Cleaning 1 (SC1) Tank, which contains 1:1:5 NH_4OH : H_2O_2 : H_2O solution and rinsed thoroughly to render the sample surface hydrophilic. The second sample was placed in DHF tank and rinsed. Hence, the second sample's surface was hydrophobic. Then both samples were dried with LuCID and were transferred to Rudolph to determine the number of stuck structures. Two types of stiction was recognizable for Rudolph during an inspection:

1. Hinge stiction (Stiction in X and Y direction)
2. Bottom stiction (Stiction in Z direction)

The Table 7.3 shows the number of structures affected by stiction for each sample.

Table 7. 3 Stiction test for hydrophilic and hydrophobic samples.

Sample	Number of stiction to the bottom (Z stiction)	Number of Hinge stiction (X-Y) stiction
1- Hydrophilic	892	2852
2- Hydrophobic	16912	10320

According to the table the hydrophilic sample has lower number of stiction in comparison with the hydrophobic surface.

7.3 - Conclusion

1. Using IPA during the drying process reduces the liquid surface tension. Therefore, in all recipes with IPA injection, the detachment lengths of cantilevers (the slope of plots) are higher than recipe with water.
2. Injecting more IPA increases the value of θ_c. This situation implies that using mixture with more concentration of IPA makes the surface of wafer more hydrophobic. Because of that, when we use 3-Times Injection recipe the surface of sample is more hydrophobic and the result from table 2 (Work of Adhesion) seems to confirm this statement.
3. Although by having 3 times IPA injection the surface layer is more hydrophobic, the measurement for detachment length shows the best result comes from 1-Time Injection. After 1-Time Injection, the value of $|\gamma_L \cos\theta_c|$ and γ_s is the lowest. Therefore the detachment length of cantilevers has the highest value and number of stiction is the minimal.
4. It is possible that the result from 1-Time Injection is related to the Marangoni effect. It means that by 1-Time Injection the Marangoni flow of the solution is higher than that of 2 or 3-Times Injection.
5. All results imply that if we want to just remove the droplet of water from the surface of a wafer, it is better to use more IPA during the drying process. However, for stiction, the

situation is more complicated. 1-Time injection shows the best result and having a less hydrophobic surface gives lesser number of structures affected by stiction. Using the mixture of water + IPA changes the solid surface properties.

Chapter 8 – Conclusion, contribution, and future works

8.1 – Summary of the thesis

In this research, we have investigated the effect of IPA in Marangoni style drying and stiction. For this purpose, we designed and fabricated two types of test wafers. One of the test wafers has micro ribbons, with a cavity beneath these ribbons. Micro-ribbons wafers give us the ability to see the effect of using IPA during a drying process. We understood that IPA is effective for drying as well as is essential to remove watermarks from the surface of wafer. We realized that increasing the number of IPA injection reduces the influence of Marangoni style drying. For this reason, we tried to find the best recipe for LuCID due to the number of IPA injection. We realized that IPA is more effective when it covers the surface of water before draining begins.

Another type of test wafer used in this research contains cantilevers with various widths and lengths. The main reason for fabrication of these tests wafers is to find out the effect of IPA on stiction. In these investigations we observed that, IPA has reduced the chance of stiction in the micro structures. Our studies show that the recipe of drying process (number of IPA injections) is very dependent on type of etchant used to release the micro structures. When the etchant was BOE, the concentration of IPA needed in the drying process should be larger than when we used DHF as an etchant.

Finally, in this research, we have investigated the role of various amount of IPA on the magnitude and the effect of both capillary forces and intersolid adhesion on stiction. The final

free or pinned state was calculated for cantilevers and this calculation was used to find the effect of IPA on stiction.

8.2 – Suggestion for future works

This study shows that different chemical materials, as an etchant, need different concentration of IPA to avoid the stiction. The relation between the surface roughness and IPA due to the stiction would be an interesting subject to work in future. This study mostly focuses on ISDP as a structural layer for the test wafers. The other materials as structural layers, commonly used in the industry need to be investigated in future.

Instead of IPA, behaviour of other liquids (e.g. Acetone or Pantene) needs to be studied further. The final part of my work implies that using a solution of two liquids can change the surface tension of solid surface during a drying process. Therefore further work needs to be done in order to determine the effect of mixture of water and IPA on the surface tension of solid surface.

Appendix I

I. ISDP

In Situ Doped Polysilicon (ISDP) films are widely used is MEMS applications. Normally ISDP is P-doped film and the amount of dopant depends on the amount of phosphine during film deposition. The morphology and resistivity of ISDP layer is totally depends on temperature and pressure in the deposition chamber [41]. Normally ISDP has low resistivity, and after annealing the resistivity decreases further.

The surface roughness of ISDP is low as well. After annealing the resistivity of film is decreasing to $\sim 1 m\Omega\text{-}cm$. This is a good advantage of ISDP to do subsequent processing step of MEMS fabrication on it.

The most important characteristic of ISDP is its high flexibility of stress control. Depending on the film deposition conditions, the layer characteristic could be change from high tensile to slight compressive. All these features make ISDP as an ideal structural material for MEMS applications.

II. LSN

Low Stress silicon Nitride (LSN) commonly is deposited by LPCVD and can be used as a structural layer for surface micromachining process. Normally the thickness of LSN is less than 1.5 μm because for more thickness it needs a long process time (high cost). In addition, if the thickness is large, the film under tensile stress will bend and even fracture [42]. At C2MI Company, the maximum LSN deposition is 500nm with ~200MPA tensile stress.

The roughness of LSN layer is very low with no porosity on the surface of the film. Annealing LSN film increases the stress level slightly. However annealing in high temperature has severe effect of crystallographic dislocation [43]. The most important characteristic of LSN is its internal tensile stress and native nonporous morphology [42]. The film density is significantly

influenced by deposition condition. LSN is another structural material in MEMS fabrication, which is widely used in semiconductor industry.

III. HF

Hydrofluoric acid (HF) is an isotropic etchant. HF is widely used in manufacturing for various MEMS devices. In this work HF was used exclusively to etch silicon oxide layer as the sacrificial layer. HF was used to remove the oxide layer from silicon and leaving hydrophobic surface. The etch rate of HF depends on concentration of HF solution. We used Diluted (10:1) HF to release cantilevers.

Before etching it is important to calculate the etch rate of DHF. For this purpose a new silicon test wafer with thermally grown oxide layer was used. First of all a thickness of oxide layer before etching was measured with N&K tool. Then the sample was placed in DHF (10:1) tank for 10 minutes. Later the sample was transferred again into N&K tool to measure the thickness of oxide layer after etching. To calculate the etch rate, the difference of oxide's thickness was calculated and was divided by the etch time. In our experiments, the etch rate of DHF (10:1) in average was 311 $\text{Å}/minute$.

IV. BOE

Buffered Oxide Etch (BOE) or buffered HF is another chemical, which is used widely in microfabrication. BOE is a mixture of buffering agent such as ammonium fluoride (NH_4F) and HF. BOE is mostly used to etch the oxide layer as a sacrificial layer. However, some oxides produce insoluble products which reduces the etch quality.

To calculate the etch rate of BOE, we did the sane procedure like HF. The thickness of annealed oxide layer was measured before and after of etching by BOE. Then the difference of thickness was divided by the timing of etching. In our experiment, the etch rate of BOE in average was 1131 $\text{Å}/minute$.

References:

[1] S. E. Lyshevski, "Nanotechnology and microtechnology, and beyond," in *Nano- and Micro-Electromechanical Systems: Fundamentals of Nano- and Microengineering, Second Edition*. CRC Press, pp. 1-16, 2005.

[2] S.F. Bart, M.W. Judy, "Micromachined devices and fabrication technology," in Enclopedia of Electronics Engineering, 1st Edition, John Wiley & Sons, pp. 648–665, 1999.

[3] N. Tas, T. Sonnenberg, H. Jansen, R. Legtenberg, and M. Elwenspoek, "Stiction in surface micromachining," *J. Micromechanics Microengineering*, vol. 6, no. 4, pp. 385–397, 1996.

[4] M. Ruths and J. N. Israelachvili, "Surface forces and nanorheology of molecularly thin films," *Handbook of Nano-technology*, 3rd Edition, Springer, pp. 857–922, 2004.

[5] U. M. Gösele, H. Stenzel, M. Reiche, T. Martini, H. Steinkirchner, and Q.-Y. Tong, "History and future of semiconductor wafer bonding," *Solid State Phenomena*, vol. 47–48. pp. 33–44, 1996.

[6] J.G. Park, S.H. Lee, J.S. Ryu, Y.K. Hong, T.G. Kim, and A.A. Busnaina, "Interfacial and electrokinetic characterization of IPA solutions related to semiconductor wafer drying and cleaning," *Journal of The Electrochemical Society*, vol. 153, pp. G811-G814, 2006.

[7] X. Xu and J. Luo, "Marangoni flow in an evaporating water droplet," *Applied Physics Letter*, vol. 91, no. 12, pp. 1-4, 2007.

[8] F. Girard, M. Antoni, and K. Sefiane, "On the effect of Marangoni flow on evaporation rates of heated water drops," *Langmuir*, vol. 24, no. 17, pp. 9207–9210, 2008.

[9] C. N. Baroud, "Marangoni convection," in Encyclopedia of Microfluidics and Nanofluidics, Springer, pp. 1705-1711, 2015.

[10] J. Eastoe and J. S. Dalton, "Dynamic surface tension and adsorption mechanisms of surfactants at the air–water interface," *Advanced in Colloid Interface Sci.*, vol. 85, no. 2–3, pp. 103–144, 2000.

[11] S. Aigo, "Spin drier for silicon wafers and the like," U.S. Patent 4 489 501, Dec. 25, 1984.

[12] K. Miya, T. Kishimoto, and A. Izumi, "Non-IPA wafer drying technology for single-spin

wet cleaning," *Electrochemical Society Proc*., vol.26, pp. 57-64, 2003.

[13] "wetbenches, " [Online]. Available: http://www.wetbenches.net. [Accessed: 9-Apr-2016].

[14] H. Akatsu, R. Hoyer, R. Ramachandran, "Method to minimize watermarks on silicon substrate, " U.S. Patent 5 932 493, Aug. 3, 1988.

[15] K. Schumacher, "Isopropyl alcohol vapor dryer system," U.S. Patent 5 054 210, oct. 8, 1991.

[16] "Ultrasonic Cleaning Equipment, The Crest Group," [Online]. Available: http://www.crest-ultrasonics.com. [Accessed: 04-Feb-2016].

[17] "substrate-drying-using-surface-tension-gradient-technology, MT System Inc.," [Online]. Available: http:// www.microtechprocess.us." [Accessed: 11-Feb-2016].

[18] "Surface Tension Gradient Dryer," [Online]. Available: http://www.microtechprocess.com/surface-tension-gradient-dryer.htm. [Accessed: 13-Feb-2016].

[19] A. C. Mitropoulos, "What is a surface excess?," *Journal of Engineering Science and Technology Review*, vol. 1, no. 1, pp. 1–3, 2008.

[20] D. K. Chattoraj and K. S. Biridi, "Adsorption at liquid Interfaces and the Gibbs Equation," in *Adsorption and the Gibbs Surface Excess*. Springer, pp. 39-82, 2012.

[21] C. H. Mastrangelo and C. H. Hsu, "Mechanical stability and adhesion of microstructures under capillary forces. I. Basic theory," *Journal of Microelectromechanical System*, vol. 2, no. 1, pp. 33–43, 1993.

[22] O. Raccurt, F. Tardif, F. A. d'Avitaya, and T. Vareine, "Influence of liquid surface tension on stiction of SOI MEMS," *Journal of Micromechanics Microengineering*, vol. 14, pp. 1083-1090, 2004.

[23] C. H. Mastrangelo and C. H. Hsu, "Mechanical stability and adhesion of microstructures under capillary forces. II. Experiments," *J. Microelectromechanical Syst*., vol. 2, no. I, pp. 44-55, 1993.

[24] G. Vhquez, E. Alvarez, and J. M. Navaza, "Tension of alcohol + water from 20 to 50 °C," Journal of *Chemical and Engineering Data,* vol. 40, no. 3, pp. 611–614, 1995.

[25] A. W. Adamson and A. P. Gast, "Friction, lubrication, and adhesion," in *Physical chemistry of surfaces*. 6th edition. Wiley, pp. 431-465, 1997.

[26] M. E. Schrader, "Young- Dupre revisited," *Langmuir*, vol. 11, no. 6, pp. 3585–3589,

1995.

[27] G. A. Lugg, "Diffusion coefficients of some organic and other vapors in air," *Analytical Chemistry*, vol. 40, no. 7, pp. 1072–1077, 1968.

[28] "Advanced 3D Wafer-Scale Packaging (WSP) Metrology System. UniFire Inc." [Online]. Available: http://www.nanometrics.com. [Accessed: 03-Mar-2016].

[29] P. de Groot, X. Colonna de Lega, J. Liesener, and M. Darwin, "Metrology of optically-unresolved features using interferometric surface profiling and RCWA modeling," *Opt. Express*, vol. 16, no. 6, pp. 3970–3975, 2008.

[30] J. Hench and Z. Strakoš, "The RCWA method-a case study with open questions and perspectives of algebraic computations," *Electronic Transaction on Numerical Analysi*, vol. 31, pp. 331–357, 2008.

[31] "N&K technology Inc. C2MI." [Online]. Available: http://www.c2mi.ca/en/content/nk-technology-inc. [Accessed: 01-Mar-2016].

[32] A. Piegari and E. Masetti, "Thin film thickness measurement: A comparison of various techniques," *Thin Solid Films*, vol. 124, no. 3–4, pp. 249–257, 1985.

[33] "Nanometrics | Film Thickness | Thin Film Metrology Reflectometry," [Online]. Available: http://www.nanometrics.com/products/reflectometry.html. [Accessed: 01-Mar-2016].

[34] "Rudolph F30-B30-E30 | C2MI." [Online]. Available: http://www.c2mi.ca/en/content/rudolph-f30-b30-e30. [Accessed: 01-Mar-2016].

[35] "3D Bump Inspection Using Laser Triangulation - Rudolph Technologies." [Online]. Available: http://www.rudolphtech.com/products/library/3d-bump-inspection-using-laser-triangulation/. [Accessed: 01-Mar-2016].

[36] F. Hadjarab and J. L. Erskine, "Image properties of the hemispherical analyzer applied to multichannel energy detection," *Journal of Electron Spectroscopy and Related Phenomena*, vol. 36, no. 3, pp. 227–243, 1985.

[37] D. W. Turner and M. I. Al Jobory, "Determination of ionization potentials by photoelectron energy measurement," *Journal of Chemical Physics*, vol. 37, no. 12, pp. 3007-3012, 1962.

[38] K. Siegbahn and K. Edvarson, "β-Ray spectroscopy in the precision range of 1 : 10," *Nucl. Phys.*, vol. 1, no. 8, pp. 137–159, Jan. 1956.

[39] "Physical Electronics - Quantera II | C2MI." [Online]. Available: http://www.c2mi.ca/en/content/physical-electronics-quantera-ii. [Accessed: 02-Mar-2016].

[40] W. N. Sharpe, B. Yuan, R. Vaidyanathan, and R. L. Edwards, "Measurements of young's modulus , poisson's ratio , and tensile strength of polysilicon," *Proceedings of the Tenth IEEE Int. Work. Microelectromechanical Syst.*, vol. 429, pp. 424–429, 1997.

[41] V. P. Lesnikova, A. S. Turtsevich, V. Y. Krasnitsky, V. A. Emelyanov, O. Y. Nalivaiko, S. V Kravtsov, and T. V Makarevich, "The structure, morphology and resistivity of in situ phosphorus doped polysilicon films," Elsevier Science, vol. 247, pp. 156–161, 1994.

[42] B. Zheng, C. Zhou, Q. Wang, Y. Chen, W. Xue, "Deposition of low stress silicon nitride thin film and its application in surface micromachining device structures," *Advanced in Material Science and Engineering*, vol. 2013, pp. 1–4, 2013.

[43] M. Tamura, H. Sunami, "Generation of dislocations induced by chemical vapor deposited Si_3N_4 films on silicon," *Japanese Journal of Applied Physics*, vol. 11, no. 8, pp. 1097–1105, 1972.